Hamiltonian in Magnetic Substances

Localized electrons systems

$$H = -2J_{ex}\Sigma_{ij} \, S_i \cdot S_j$$

$J_{ex} < 0$ （in case of wave functions mixed）

: Antiferromagnetism

$J_{ex} > 0$ （in case of wave functions orthgonalized）

: Ferromagnetism

Magnetism in Localized Electrons Systems

Paramagnetism   **Ferromagnetism**   **Antiferromagnetism**

(a)

(b)

J
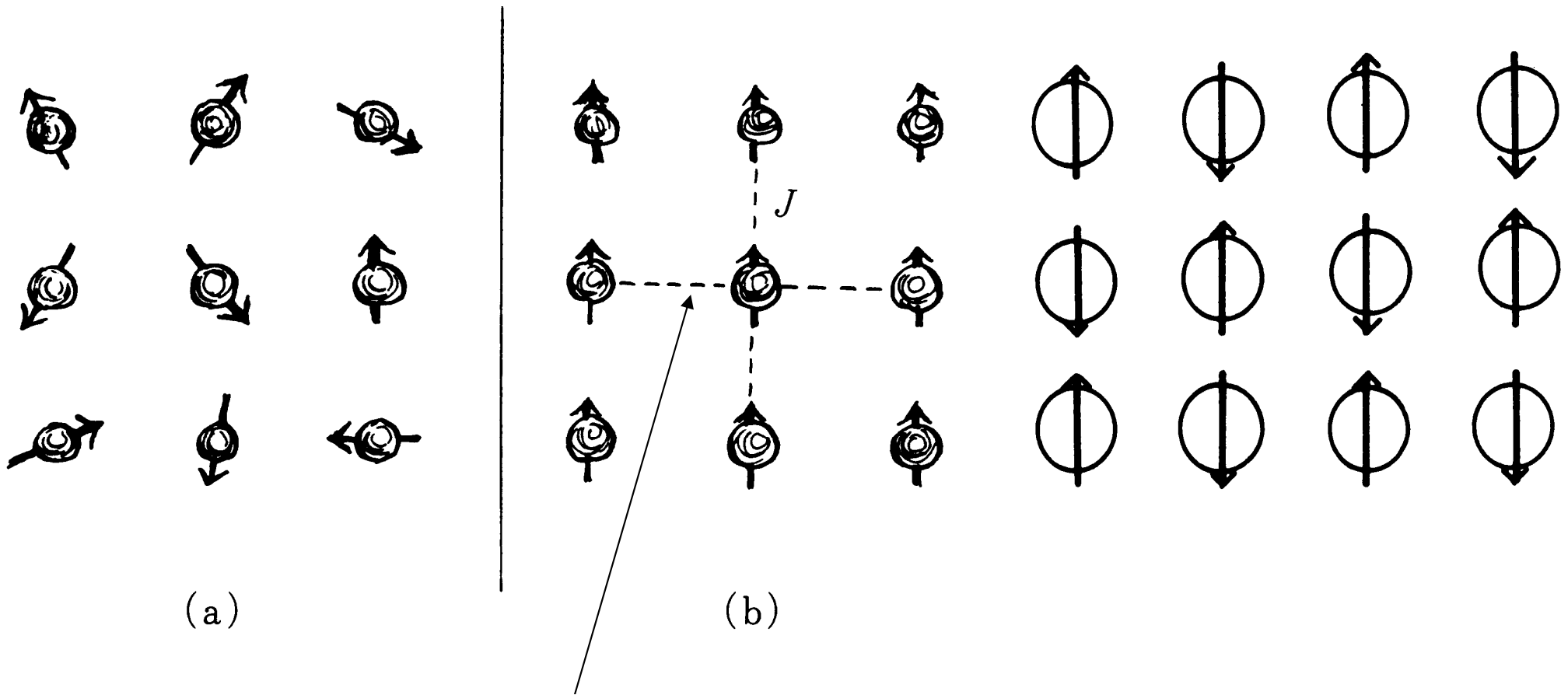
Quantum mechanical Exchange interaction J_{ex}

Periodic Table for atomic element

（基底状態の中性原子の外殻電子配置）

原子およびイオンの電子配置を示す記号については
すべての初歩的な原子物理学の教科書において述べ
られている．文字 s , p , d …は $\hbar$ を単位とする軌道
角モーメント0,1,2,をもっている電子を示す．文字
の左側の数字は軌道の主量子数を示す．右肩上の数
字は…

3d Transition elements

4f Rare earth elements

| H¹ | | | | | | | | | | | | | | | | | | He² |

H¹ $1s$ — He² $1s^2$

| Li³ $2s$ | Be⁴ $2s^2$ | | | | | | | | | | | B⁵ $2s^2 2p$ | C⁶ $2s^2 2p^2$ | N⁷ $2s^2 2p^3$ | O⁸ $2s^2 2p^4$ | F⁹ $2s^2 2p^5$ | Ne¹⁰ $2s^2 2p^6$ |

Na¹¹ $3s$ — Mg¹² $3s^2$ — Al¹³ $3s^2 3p$ — Si¹⁴ $3s^2 3p^2$ — P¹⁵ $3s^2 3p^3$ — S¹⁶ $3s^2 3p^4$ — Cl¹⁷ $3s^2 3p^5$ — Ar¹⁸ $3s^2 3p^6$

K¹⁹ $4s$ — Ca²⁰ $4s^2$ — Sc²¹ $3d\,4s^2$ — Ti²² $3d^2\,4s^2$ — V²³ $3d^3\,4s^2$ — Cr²⁴ $3d^5\,4s$ — Mn²⁵ $3d^5\,4s^2$ — Fe²⁶ $3d^6\,4s^2$ — Co²⁷ $3d^7\,4s^2$ — Ni²⁸ $3d^8\,4s^2$ — Cu²⁹ $3d^{10}\,4s$ — Zn³⁰ $3d^{10}\,4s^2$ — Ga³¹ $4s^2 4p$ — Ge³² $4s^2 4p^2$ — As³³ $4s^2 4p^3$ — Se³⁴ $4s^2 4p^4$ — Br³⁵ $4s^2 4p^5$ — Kr³⁶ $4s^2 4p^6$

Rb³⁷ $5s$ — Sr³⁸ $5s^2$ — Y³⁹ $4d\,5s^2$ — Zr⁴⁰ $4d^2\,5s^2$ — Nb⁴¹ $4d^4\,5s$ — Mo⁴² $4d^5\,5s$ — Tc⁴³ $4d^6\,5s$ — Ru⁴⁴ $4d^7\,5s$ — Rh⁴⁵ $4d^8\,5s$ — Pd⁴⁶ $4d^{10}$ — Ag⁴⁷ $4d^{10}\,5s$ — Cd⁴⁸ $4d^{10}\,5s^2$ — In⁴⁹ $5s^2 5p$ — Sn⁵⁰ $5s^2 5p^2$ — Sb⁵¹ $5s^2 5p^3$ — Te⁵² $5s^2 5p^4$ — I⁵³ $5s^2 5p^5$ — Xe⁵⁴ $5s^2 5p^6$

Cs⁵⁵ $6s$ — Ba⁵⁶ $6s^2$ — La⁵⁷ $4f\,5d\,6s^2$ — Hf⁷² $4f\,5d^2\,6s^2$ — Ta⁷³ — W⁷⁴ — Re⁷⁵ — Os⁷⁶ — Ir⁷⁷ — Pt⁷⁸ — Au⁷⁹ — Hg⁸⁰ $5d^{10}\,6s^2$ — Tl⁸¹ $6s^2 6p$ — Pb⁸² $6s^2 6p^2$ — Bi⁸³ $6s^2 6p^3$ — Po⁸⁴ $6s^2 6p^4$ — At⁸⁵ $6s^2 6p^5$ — Rn⁸⁶ $6s^2 6p^6$

Fr⁸⁷ $7s$ — Ra⁸⁸ $7s^2$ — Ac⁸⁹ $6d\,7s^2$

Ce⁵⁸ $4f^2\,6s^2$ — Pr⁵⁹ $4f^3\,6s^2$ — Nd⁶⁰ $4f^4\,6s^2$ — Pm⁶¹ $4f^5\,6s^2$ — Sm⁶² $4f^6\,6s^2$ — Eu⁶³ $4f^7\,6s^2$ — Gd⁶⁴ $4f^7\,5d\,6s^2$ — Tb⁶⁵ $4f^8\,5d\,6s^2$ — Dy⁶⁶ $4f^{10}\,6s^2$ — Ho⁶⁷ $4f^{11}\,6s^2$ — Er⁶⁸ $4f^{12}\,6s^2$ — Tm⁶⁹ $4f^{13}\,6s^2$ — Yb⁷⁰ $4f^{14}\,6s^2$ — Lu⁷¹ $4f^{14}\,5d\,6s^2$

Th⁹⁰ $6d^2\,7s^2$ — Pa⁹¹ $5f^2\,6d\,7s^2$ — U⁹² $5f^3\,6d\,7s^2$ — Np⁹³ $5f^4\,7s^2$ — Pu⁹⁴ $5f^6\,7s^2$ — Am⁹⁵ $5f^7\,7s^2$ — Cm⁹⁶ $5f^7\,6d\,7s^2$ — Bk⁹⁷ — Cf⁹⁸ — Es⁹⁹ — Fm¹⁰⁰ — Md¹⁰¹ — No¹⁰² — Lr¹⁰³

1. Either *d*- or *f*- shell electrons wave functions are distributed at closer location to nuclei than either *s*- or *p*- shell are.

2. Angular dependence of *d*- and *f*- wave functions are so complicated that their contirbution to covalent bonding is not so significant

What is *L-S* multiplet ? Consider two electrons on either p or d shells.

Electron-electron interaction lifts such the degeneracy as $_6C_2=15$ for *p* shell and $_{10}C_2=45$ for *d* shell. Eigen energy at each state with two electrons is given as follows ;

$$E_p(\uparrow\downarrow) = 2E_p^0 + U \; > \; E_p(\uparrow\uparrow, \leftarrow\leftarrow, \downarrow\downarrow)$$

$$= 2E_p^0 + U - J_{ex} \;\; \text{(because of } J_{ex} > 0\text{)}$$

↑↓
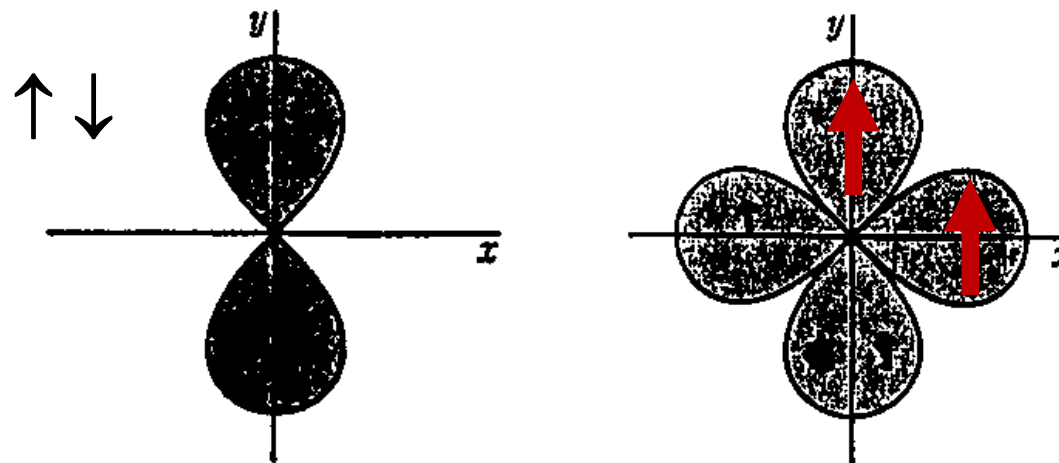
(a) p_y に2個   (b) p_x, p_y にそれぞれ1個

図 2-3　2個の *p* 電子が存在するときの電子分布

When J_{ex} is negative due to the overlap of wave functions among nearest neighbor atomic sites, Spins are anti-parallel. On the other hand, if the wave function is orthogonalized, J_{ex} is always positive and hence ferromagnetic coupling is realized

Proof:

$$J_{n_1 n_2} = \int \varphi_{n_1}^*(r_1) \varphi_{n_2}^*(r_2) \frac{e^2}{r_{12}} \varphi_{n_1}(r_2) \varphi_{n_2}(r_1) d\tau_1 d\tau_2$$

1 / r is expanded in a Fourier series as

$$\frac{e^2}{r_{12}} = \frac{1}{V} \sum_k \frac{4\pi e^2}{k^2} e^{ik\cdot(r_1 - r_2)}$$
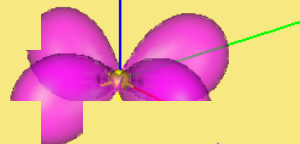
J_{ex} = −2St + J' = J' (because of S=0)

$$J_{n_1 n_2} = \frac{1}{V} \sum_k \frac{4\pi e^2}{k^2} \int \varphi_{n_1}^*(r_1) \varphi_{n_2}(r_1) e^{ik\cdot r_1} d\tau_1$$

$$\times \int \varphi_{n_2}^*(r_2) \varphi_{n_1}(r_2) e^{-ik\cdot r_2} d\tau_2 > 0$$

のように書きかえられる．したがって $J_{n_1 n_2}$ は常に正である．

いろいろな軌道：電子の存在確率

s軌道

d軌道
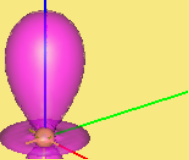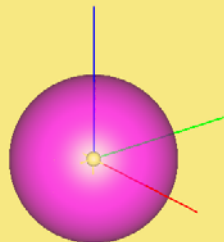
p軌道
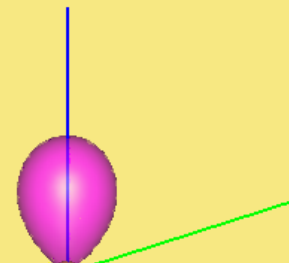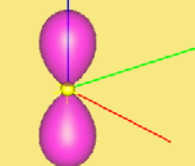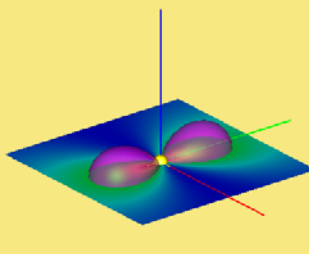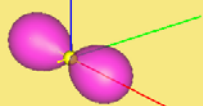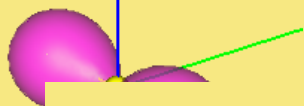
d軌道

(2) Real number representation of 3d wave functions

(1) Complex number representation of 3d wave functions

3d orbitals

e_g orbitals

$3d^9 : S=1/2$

$3d^4 : S=2$

$3z^2 - r^2$

$x^2 - y^2$

t_{2g} orbitals

zx

yz

xy
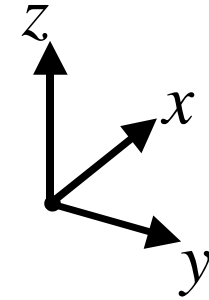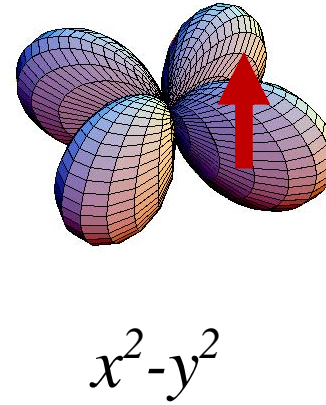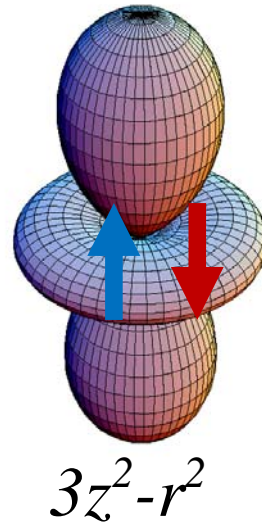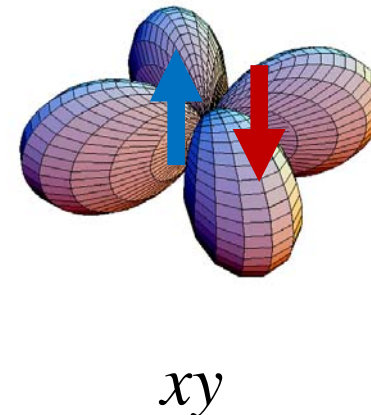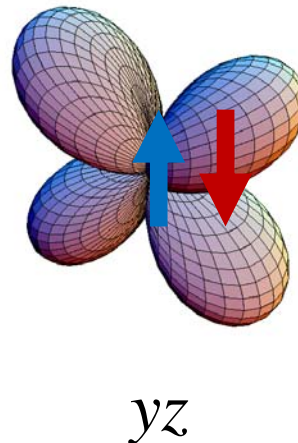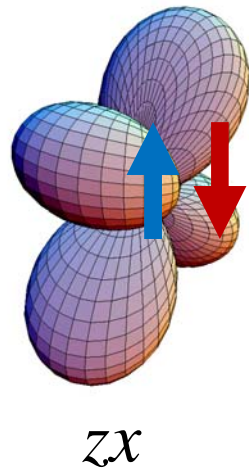
$$E_d(\uparrow\downarrow) = 2E_d^0 + U > E_d(\uparrow\uparrow, \leftarrow\leftarrow, \downarrow\downarrow) = 2E_d^0 + U - J_{ex} \text{ (because of } J_{ex} > 0)$$

Electronic state for unoccupied shell is classified by four quantum numbers (L, M_L, S, M_S)

L : Magnitude of total orbital angular momentum, M_L : z-component of L

S : Magnitude of total spin momentum, M_S : z-component of S

LS multiplet : when L and S are given, a number states of $(2L+1)(2S+1)$ are possible. What is the ground state for numbers of S and L with a lowest eigen energy ?

Hund's rule is applied to determine the ground state in *LS* multiplets ;

1. the maximum S among possible configurations, at the same time,

2. the state possesses the maximum L.

How to obtain the total angular momentum *J* from *S* and *L*

Spin-orbit interaction makes *LS* multiples split into the *J* multiplets for *J=S+L*

$$J=L+S, \ L+S-1, \ \cdot \ \cdot \ \cdot, \ |L-S|$$

Qualitative interpretation of spin-orbit interaction:

Electron spin feels magnetic field generated by current *I* due to orbital motions of the nuclei with positive charge of *Ze* (Biot-Savart'law)

$$H \sim [r \times I] / r^3 \sim l / r^3$$

$$\zeta \, l \cdot s$$

$$g\mu_B s \cdot H_{ze} = g\mu_B s \cdot Z\mu_B l < \frac{1}{r^3} >_{AV} = 2\mu_B^2 Z < \frac{1}{r^3} >_{AV} l \cdot s = \zeta l \cdot s$$

$$\zeta = \frac{1}{2} Z \left(\frac{e\hbar}{mc} \right)^2 < \frac{1}{r^3} >_{AV}$$

$$\mu_s = -g \left(\frac{e\hbar}{2mc} \right) s \qquad \mu_0 = -\frac{e}{c} \cdot \frac{1}{2} [r \times v] = -\frac{e}{2mc} [r \times mv]$$

$$\mu_0(H=0) = -\frac{e}{2mc} [r \times p] = -\frac{e\hbar}{2mc} l = -\mu_B l$$

Spin-orbit interaction : $\mathcal{H}_{sl} = \sum_i \zeta \, l_i \cdot s_i$

Effective Hamiltonian of spin – orbit interaction on the basis of Hund's Rule

$$(\mathcal{H}_{sl})_{LS} = \mathcal{H}_{LS} = \lambda \, \mathbf{L} \cdot \mathbf{S}$$

Less than half in orbital shell : $n < 2l+1$

$s_i = S/n$

d orbital : $n < 5$

f orbital : $n < 7$

More than half in orbital shell : $n > 2l+1$

$s_i = -S/[2(2l+1) - n]$

d orbital : $n > 5$

f orbital : $n > 7$

$$\mathcal{H}_{sl} = \Sigma_i \zeta l_i \cdot S/n = \zeta/n(\Sigma_i l_i) \cdot S = (\zeta/n)L \cdot S$$

$$\lambda = \zeta/n > 0$$

$$n > 2l+1 : \lambda = -\zeta/(4l+2-n) < 0$$

$$n = 2l+1 : L=0, \ S=(2l+1)/2 \rightarrow H_{sl}=0$$

表 2-3　スピン軌道相互作用の定数

	電子数	電子状態	$\lambda \, \mathrm{cm^{-1}}$
Ti^{3+}	d^1	^2D	154
V^{3+}	d^2	^3F	104
Cr^{3+}	d^3	^4F	87
Mn^{3+}	d^4	^5D	85
V^{2+}	d^3	^4F	55
Cr^{2+}	d^4	^5D	57
Fe^{2+}	d^6	^5D	-100
Co^{2+}	d^7	^4F	-180
Ni^{2+}	d^8	^3F	-335
Cu^{2+}	d^9	^2D	-828

The **J** value among **J** multiplets is detemined so as to have a lowest energy on the spin-orbit interaction

$$\lambda L \cdot S = \frac{1}{2}\lambda(J^2 - L^2 - S^2)$$

$$(\lambda L \cdot S)_J = \frac{1}{2}\lambda\{J(J+1) - L(L+1) - S(S+1)\}$$

Using the Heisenberg equation :

$$\frac{d\vec{A}}{dt} = \frac{i}{\hbar}[H, \vec{A}] = \frac{i}{\hbar}(H\vec{A} - \vec{A}H)$$

Prove that

$$\hbar\frac{dL}{dt} = \lambda[S \times L] = \lambda[J \times L]$$

$$\hbar\frac{dS}{dt} = \lambda[L \times S] = \lambda[J \times S]$$

J

S
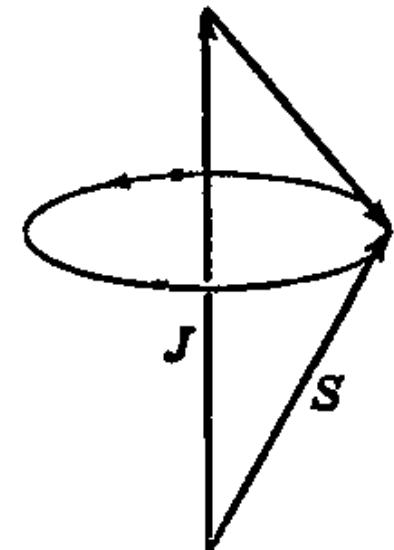
L S と J

$$J = L + S$$

$$L = aJ + bJ_\perp \,, \quad S = (1-a)J + cJ_\perp$$

Therefore,

$$J \cdot L = L^2 + S \cdot L$$

$$J \cdot L = aJ^2 \quad a = [L^2 + S \cdot L]/J^2 = [L^2 + (J^2 - L^2 - S^2)/2]/J^2 = (J^2 + L^2 - S^2)/2J^2$$

$$a = \frac{1}{2J(J+1)}\{J(J+1) + L(L+1) - S(S+1)\}$$

Total magnetic moment is derived in tems of projected components of **S** and **L** along **J**

$$\mu = -\mu_B(L + 2S) = -\mu_B(2-a)J = -g_J \mu_B J$$

$$g_J = \frac{3}{2} + \frac{S(S+1) - L(L+1)}{2J(J+1)}$$

g_J: Lande's g factor

Paramagnetism and the Curie law of magnetic susceptibility

When magnetic field is applied along the z-axis, the Zeeman energy is given by

$$E(J, M_J) = g_J \mu_B H M_J$$

The occupation probability at this eigen state at temperature T is expressed in terms of a Boltzmann distribution as

$$\sim \exp\{-E(J, M_J)/kT\}$$

Then, the thermal equilibrium is obtained as follows

$$M(H, T) = \frac{N\left\{\sum_{M_J=-J}^{J}(-g_J\mu_B M_J)\exp(-g_J\mu_B HM_J/kT)\right\}}{\left\{\sum_{M_J=-J}^{J}\exp(-g_J\mu_B HM_J/kT)\right\}}$$

N : avodadro number, k_B : Boltzmann constant

Prove the following formula ;

$$M(H, T) = N g_J \mu_B J \; B_J\left(\frac{J g_J \mu_B H}{kT}\right)$$

$$B_J(x) = \frac{2J+1}{2J} \coth \frac{2J+1}{2J}x - \frac{1}{2J} \coth \frac{x}{2J}$$

$B_J(x)$: **Brillouin** function

$x \to 0$: $B_J(x) \to (J+1)/3J \cdot x$

$x \to \infty$: $B_J(x) \to 1$

Curie Law for
Paramagnetic materials

$H/T \to 0$: $M \to (C/T) \cdot H$

$H/T \to \infty$: $M \to N g_J \mu_B J$

Saturation
magnetization

Calculate the Curie constant C

Here you find the following definition

$$\coth x = \frac{\cosh x}{\sinh x} \sim \frac{1 + \frac{x^2}{2}}{x + \frac{x^3}{6}} = \frac{1}{x}\left(1 + \frac{x^2}{2}\right)\left(1 + \frac{x^2}{6}\right)^{-1}$$

$$\sim \frac{1}{x}\left(1 + \frac{x^2}{2}\right)\left(1 - \frac{x^2}{6}\right) \sim \frac{1}{x}\left(1 - \frac{x^2}{6} + \frac{x^2}{2}\right) = \frac{1}{x} + \frac{x}{3}$$

$$\therefore B_S(x) \sim \frac{2S+1}{2S}\left[\frac{2S}{2S+1}\frac{1}{x} + \frac{1}{3}\frac{2S+1}{2S}x\right] - \frac{1}{2S}\left[\frac{2S}{x} + \frac{1}{3}\frac{x}{2S}\right]$$

$$= \frac{1}{3}\left(\frac{2S+1}{2S}\right)^2 x - \frac{1}{3}\left(\frac{1}{2S}\right)^2 x = \frac{S+1}{3S}x$$

4*f* electrons does not so strongly interact with surrounding ions,
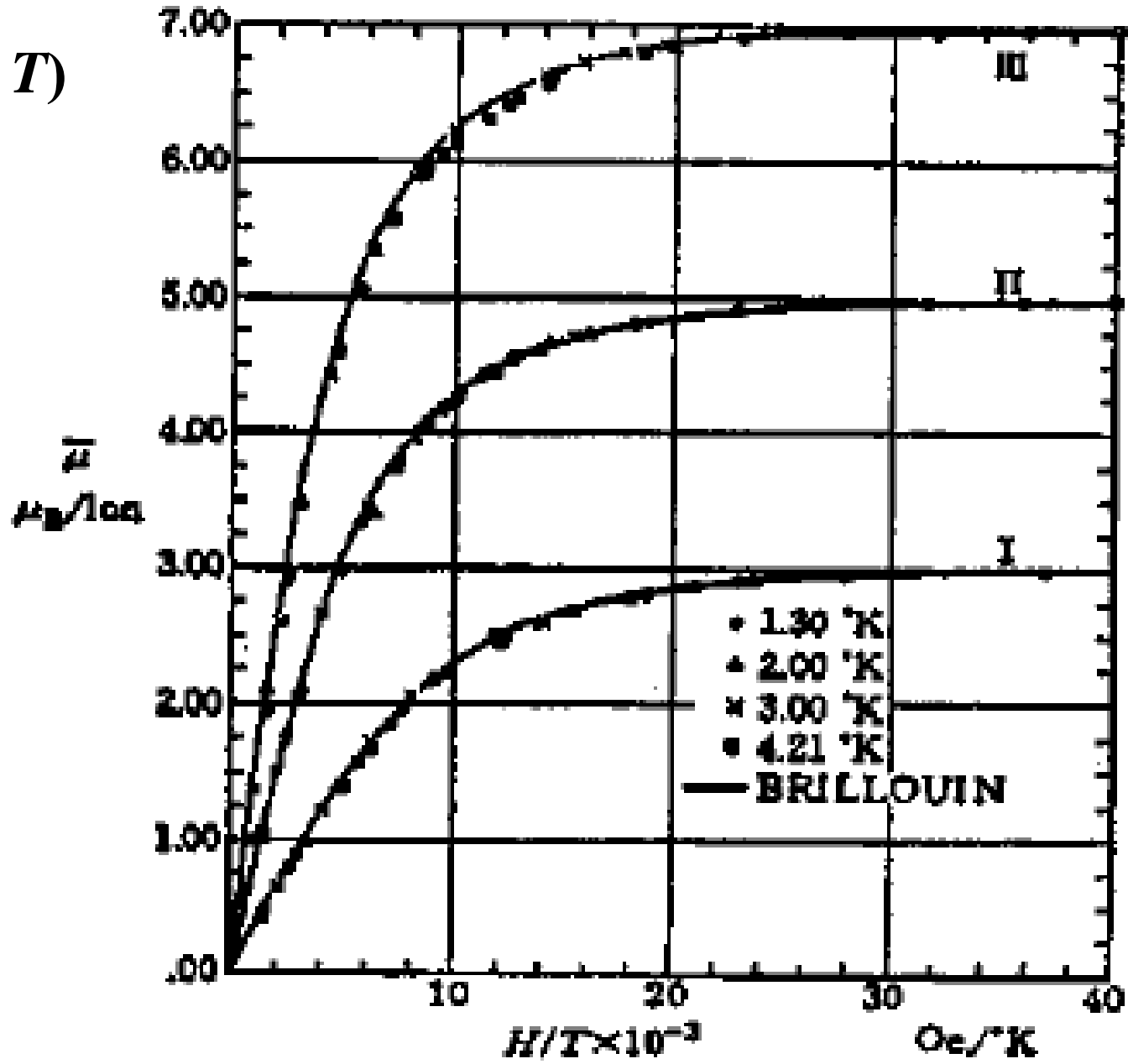
keeping their localized character.

Therefore, the magnetic moment per ion is described in terms of J.

To confirm this, the theoretical value is compared with the experimental value

$$p = g_J\sqrt{J(J+1)} \; \text{:} \; \text{Effective moments}$$

$$\chi(T) = (N\mu_B^2/3k_BT)p^2$$

表 2-4　希土類元素の有効ボーア磁子数

イ　オ　ン	f^n	基底状態	EXP	thery $^+$	thery $^{++}$
La^{3+}	f^0	^1S	dia	0.00	0.00
Ce^{3+}	f^1	$^2F_{5/2}$	2.5	2.54	2.56
Pr^{3+}	f^2	$^3H_4$	3.6	3.58	3.62
Nd^{3+}	f^3	$^4I_{9/4}$	3.8	3.62	3.68
Pm^{3+}	f^4	$^5I_4$	—	2.68	2.83
Sm^{3+}	f^5	$^6H_{5/2}$	1.5	0.84	1.55
Eu^{3+}	f^6	$^7F_0$	3.6	0.00	3.40
Gd^{3+}	f^7	$^8S_{7/2}$	7.9	7.94	7.94
Tb^{3+}	f^8	$^7F_6$	9.7	9.72	9.7
Dy^{3+}	f^9	$^6H_{15/2}$	10.5	10.63	10.6
Ho^{3+}	f^{10}	$^5I_8$	10.5	10.60	10.6
Er^{3+}	f^{11}	$^4I_{15/2}$	9.4	9.59	9.6
Tm^{2+}	f^{12}	$^3H_6$	7.2	7.57	7.6
Yb^{3+}	f^{13}	$^2F_{7/2}$	4.5	4.54	4.5
Lu^{3+}	f^{14}	^1S	dia	0.00	0.00

† （2-31）式から基底状態の g_J を用い $g_J\sqrt{J(J+1)}$ を計算したもの。

†† （2-32）式を用い常温付近の p（有効ボーア磁子）を計算したもの（Van Vleck-Franck）。

Magnetic moments of ions in the crystal

$3d$ electrons in the d shell are strongly interacted with the surrounding crystal electric field potential

Orbital moment is quenched, confirmed experimentally by the following results

表 2-5　遷移元素　特に鉄族イオンの有効ボーア磁子
電子配置の後の記号は最低エネルギーの状態の L, S, J を示す
$(^{2S+1}L_J)$。

電子構造	イオン	p 実験値	$g_J\sqrt{J(J+1)}$	$\sqrt{4S(S+1)}$
$3d^1\ ^2D_{1/2}$	Ti^{3+}		1.55	1.73
	V^{4+}	1.8	1.55	1.73
$3d^2\ ^3F_2$	V^{3+}	2.8	1.63	2.83
$3d^3\ ^4F_{3/2}$	V^{2+}	3.8	0.77	3.87
	Cr^{3+}	3.7	0.77	3.87
	Mn^{4+}	4.0	0.77	3.87
$3d^4\ ^5D_0$	Cr^{2+}	4.8	0	4.90
	Mn^{3+}	5.0	0	4.90
$3d^5\ ^6S_{5/2}$	Mn^{2+}	5.9	5.92	5.92
	Fe^{3+}	5.9	5.92	5.92
$3d^6\ ^5D_4$	Fe^{2+}	5.4	6.70	4.90
$3d^7\ ^4F_{9/2}$	Co^{2+}	4.8	6.54	3.87
$3d^8\ ^3F_4$	Ni^{2+}	3.2	5.59	2.83
$3d^9\ ^2D_{5/2}$	Cu^{2+}	1.9	3.55	1.73

(1) Complex number representation of 3d wave functions :

$$R_{32}(r)\, Y_2^m(\theta, \varphi) \quad (m = -2, -1, 0, 1, 2)$$

(2) Real number representation of 3d wave functions :

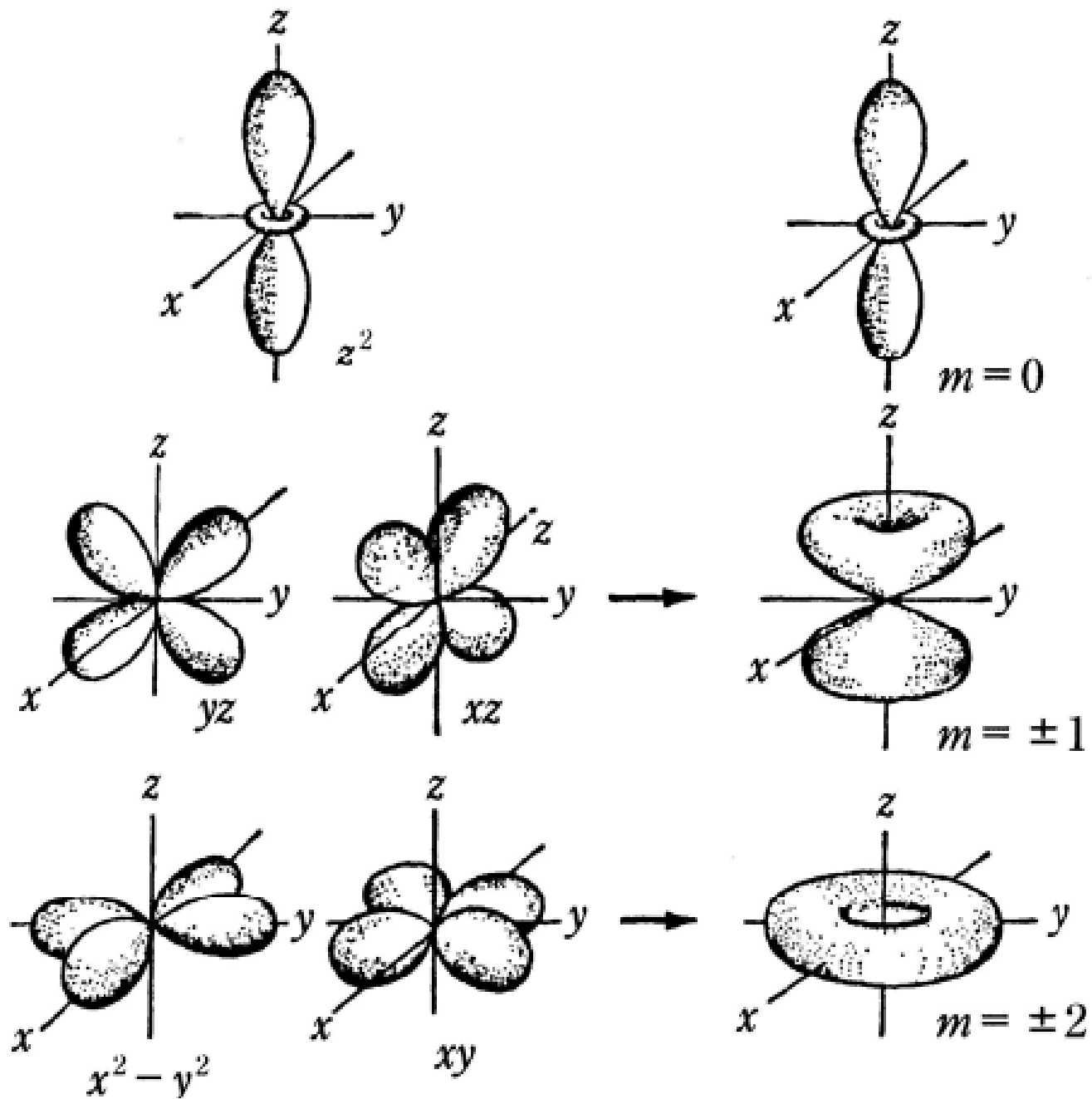$d\varepsilon$ 軌道 : $d_{xy} = f(r) \cdot xy, \quad d_{yz} = f(r) \cdot yz, \quad d_{zx} = f(r) \cdot zx$

$d\gamma$ 軌道 : $d_{x^2-y^2} = f(r)(x^2 - y^2), \quad d_{z^2} = \dfrac{1}{\sqrt{2}} f(r)(3z^2 - r^2)$

We have the following relation between the representations of above (1) and (2)

$$d_{z^2} = R(r) r^2 Y_2^0(\theta, \phi), \quad d_{yz} = -R(r)\frac{r^2}{\sqrt{2}\, i}(Y_2^1 + Y_2^{-1})$$

$$d_{zx} = -R(r)\frac{r^2}{\sqrt{2}\, i}(Y_2^1 - Y_2^{-1}), \quad \boxed{d_{x^2-y^2} = R(r)\frac{r^2}{\sqrt{2}}(Y_2^2 + Y_2^{-2})}$$

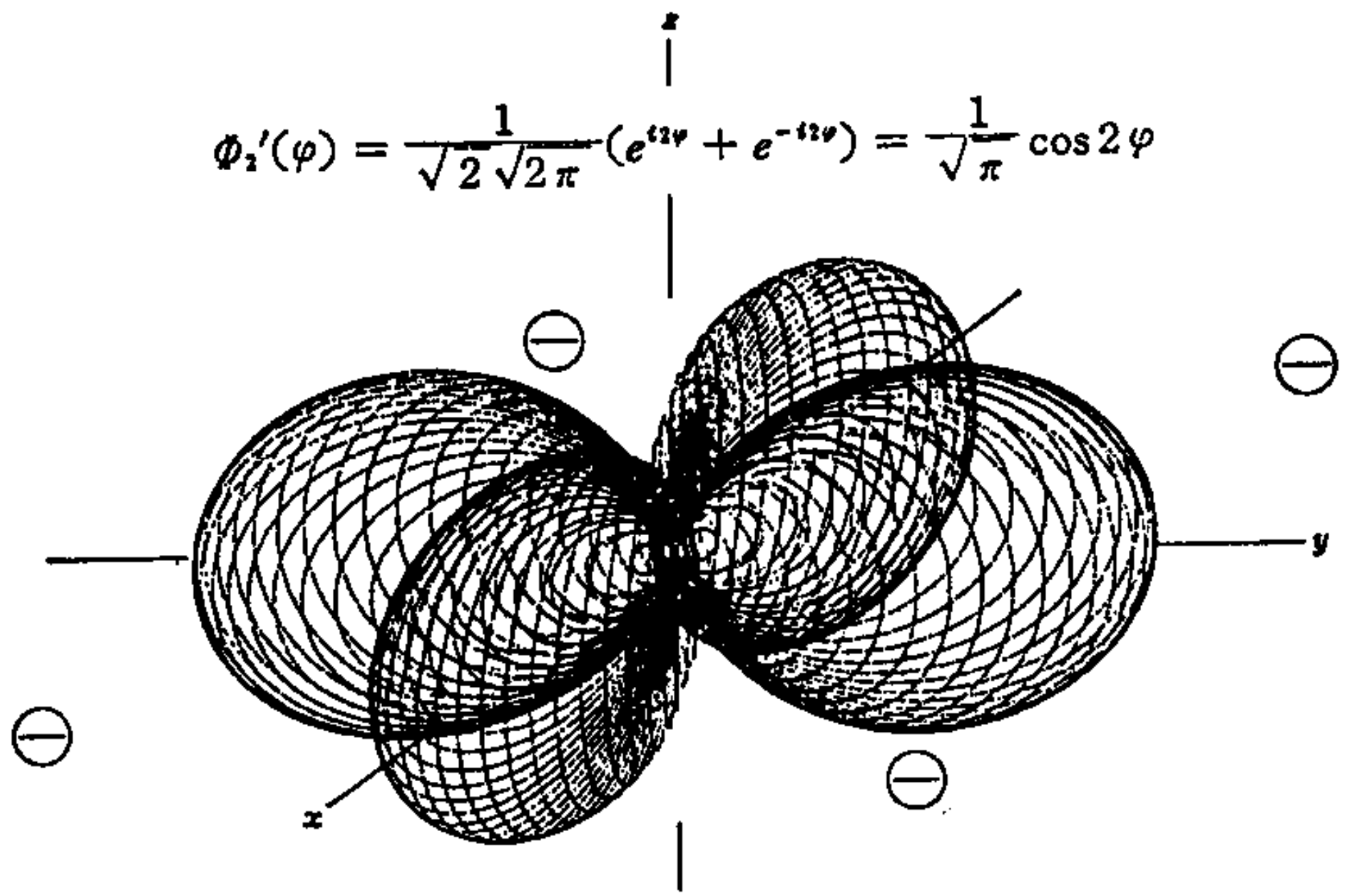$$d_{xy} = R(r)\frac{r^2}{\sqrt{2}\, i}(Y_2^2 - Y_2^{-2})$$

(2) Real number representation of 3d wave functions

(1) Complex number representation of 3d wave functions

$$\Phi_2{}'(\varphi) = \frac{1}{\sqrt{2}\sqrt{2\pi}}(e^{i2\varphi} + e^{-i2\varphi}) = \frac{1}{\sqrt{\pi}}\cos 2\varphi$$

What is the origin of crystal electric field

Electric field produced by surrounding ions acts on electrons in the _d_ shell.

Crystal field potential is given by $H_{crys}=\sum_i V_{cr}(r_i)$

For example, we consider the magnetic ions surrounded by octahedral oxygen ions which is displayed as follow :

Which electron's wave function is in a state with eigen energy lower than the other ?

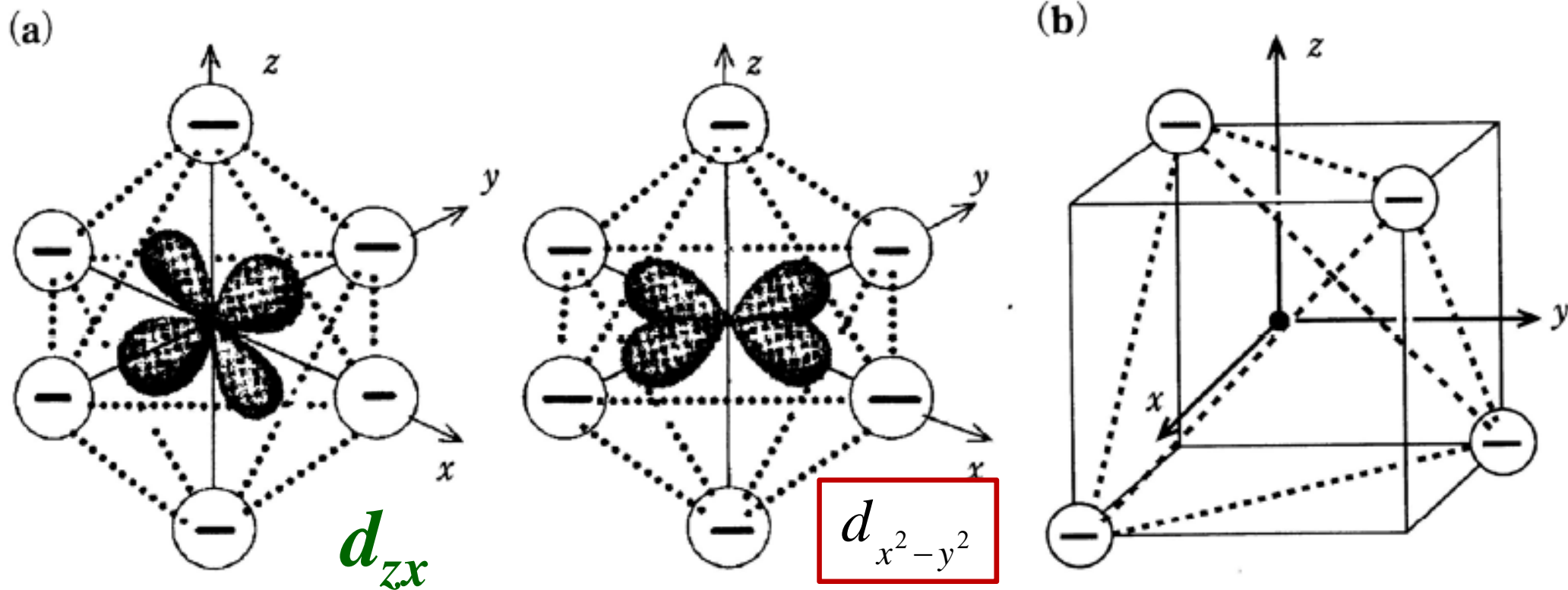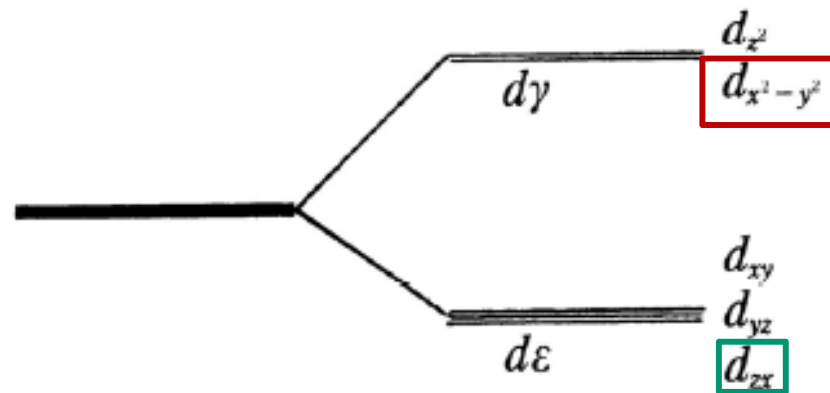$d\varepsilon$ 軌道 $d(zx)$ を示す $d\gamma$ 軌道 $d(x^2-y^2)$ を示す

正八面体的結晶場と d 軌道

(a)

d_{zx}

$d_{x^2-y^2}$

(b)
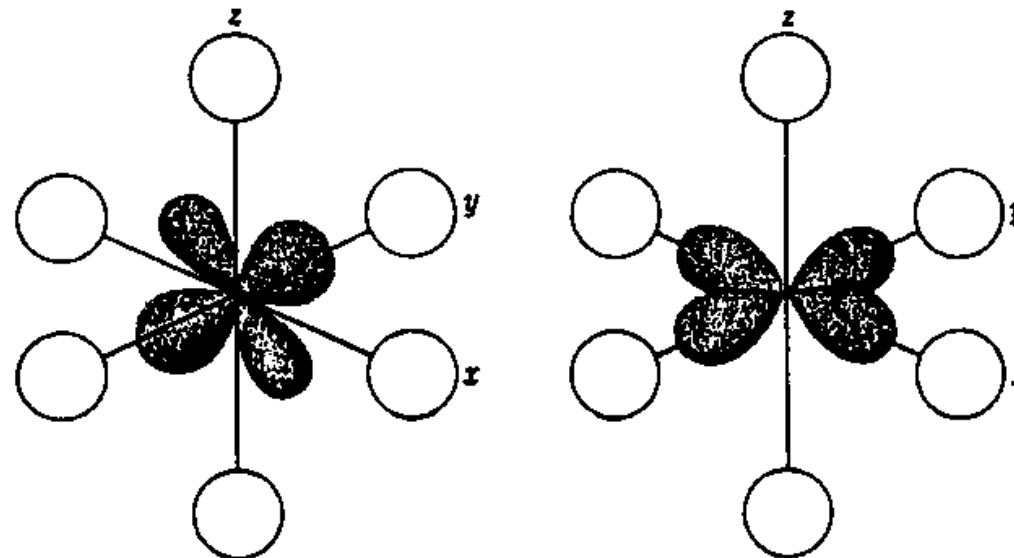
図 3-4　（a）正8面体配置と d 軌道（左は d_{zx} 軌道，右は $d_{x^2-y^2}$ 軌道. $d_{x^2-y^2}$ 軌道は−イオンの方向へ伸びているのでエネルギーが高い）．（b）4面体配置（●中心イオンと−イオンの位置のみを示す）

$d\gamma$　　d_{z^2}
　　$d_{x^2-y^2}$

d_{xy}
d_{yz}
$d\varepsilon$　　d_{zx}

Here, we see that a real representation of wave function results in $<l_z>= 0$, as an example for the case of

$$d_{xy}=R(r)\frac{r^2}{\sqrt{2}\,i}(Y_2^2-Y_2^{-2})$$

It is proved that this wave function is not an eigen-state for l_z from the relation

$$l_z d_{xy}=R(r)\frac{r^2}{\sqrt{2}\,i}l_z(Y_2^2-Y_2^{-2})=2R(r)\frac{r^2}{\sqrt{2}\,i}(Y_2^2+Y_2^{-2})\neq d_{xy}$$

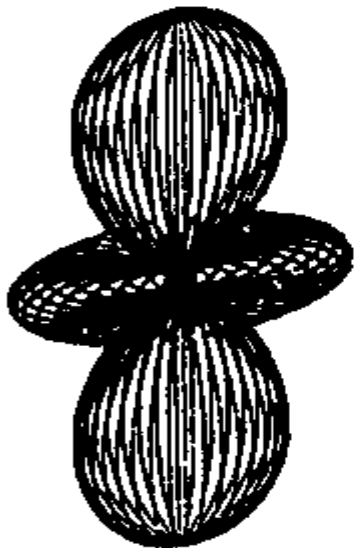In fact, $<l_z>= 0$ is valid from the following calculations;

$$<l_z>=\int_0^\infty r^6 R^2(r)dr\cdot\int_0^\pi\int_0^{2\pi}(Y_2^2-Y_2^{-2})^*\ l_z(Y_2^2-Y_2^{-2})\sin\theta\ d\theta d\phi$$

$$=2\int_0^\infty r^6 R^2(r)dr\cdot\iint(Y_2^{-2}-Y_2^2)(Y_2^2+Y_2^{-2})\sin\theta\ d\theta d\phi = 0$$

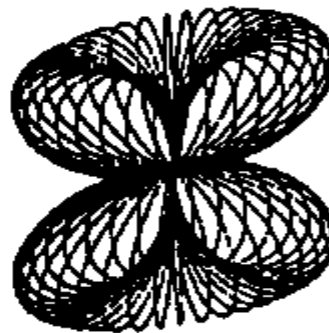**The orbital moment is quenched in case of the degeneracy being lifted up.**

Because the wave function is described by the real component, we have the following relation :

$$l = (\hbar/i)[r \times \text{grad}]$$

$$\langle L \rangle_{Av} = \int \Psi \, L\Psi \, d\tau = \int \Psi^* L\Psi^* d\tau$$

$$= -\left\{ \int \Psi \, L\Psi \, d\tau \right\}^* = -\langle L \rangle_{Av}^*$$

d
m=0

d
m=1

d
m=2

We consider the following case :

d^6: Fe^{3+}, Co^{2+}

$$V_{cr} < V_H$$
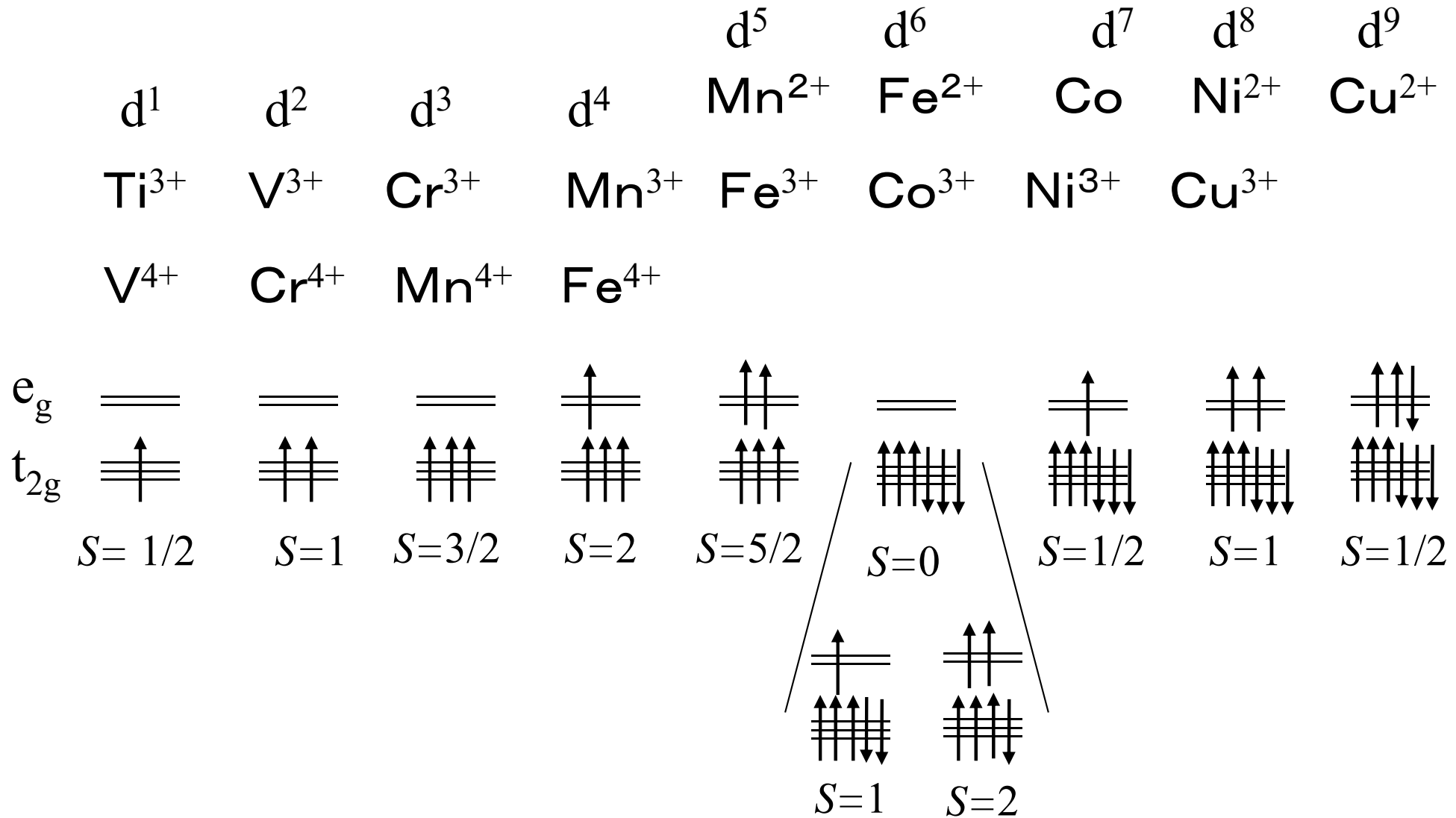
$$V_{cr} > V_H$$

(a) high spin state   (b) low spin state
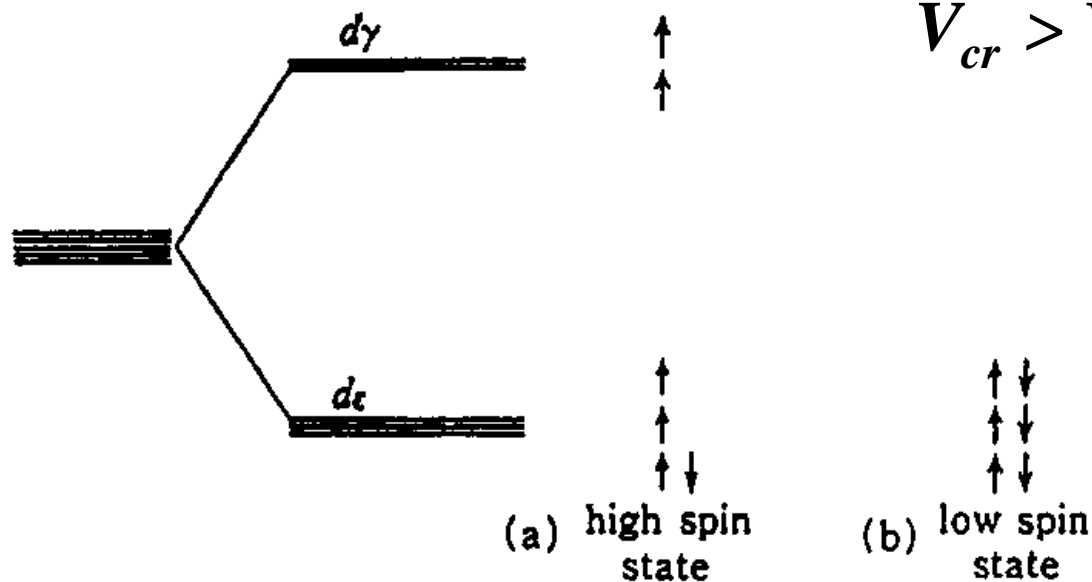
high spin state と low spin state での電子の

配置 d^6 の場合

Electron Configuration in Transition Metal Ions
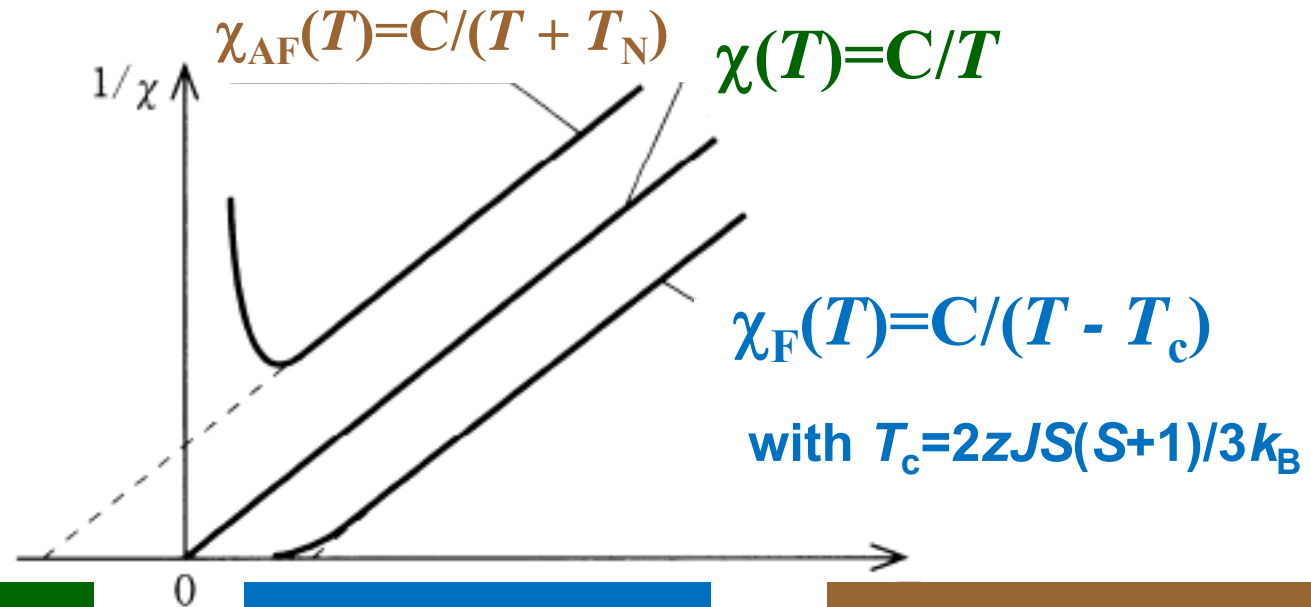
Hunds' rule and Crystal Electric Field Effect

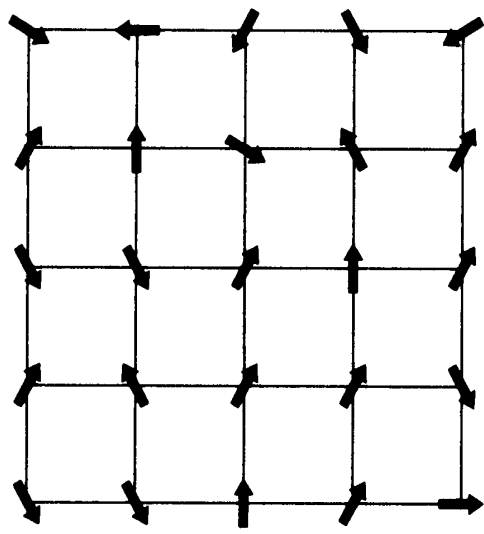## Problem 7

1. $3d^3$ ($S= ?$, $L= ?$, $J= ?$, $E_{SL}= ?$)

2. $4f^8$ ($S= ?$, $L= ?$, $J= ?$, $E_{SL}= ?$)

Temperature variation of susceptibility for localized systems

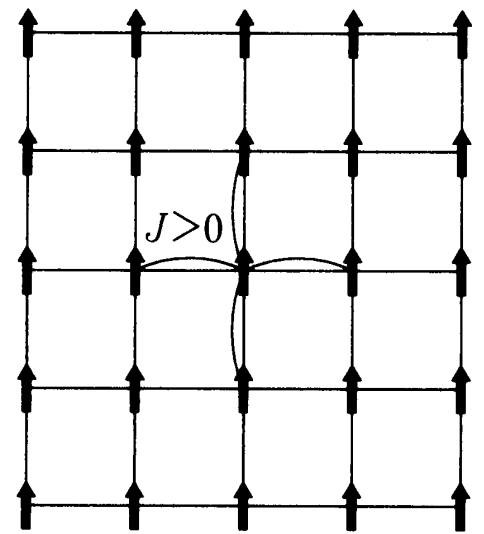$$\chi_{AF}(T)=C/(T + T_N)$$
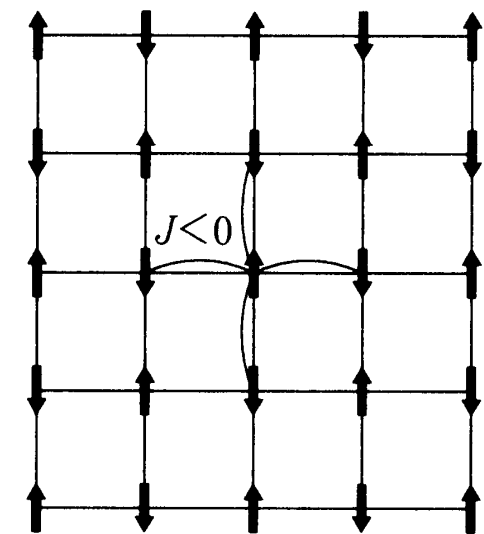
$$\chi(T)=C/T$$

$$\chi_F(T)=C/(T - T_c)$$

with $T_c = 2zJS(S+1)/3k_B$

Paramagnetism

Ferromagnetism

AntiFerromagnetism

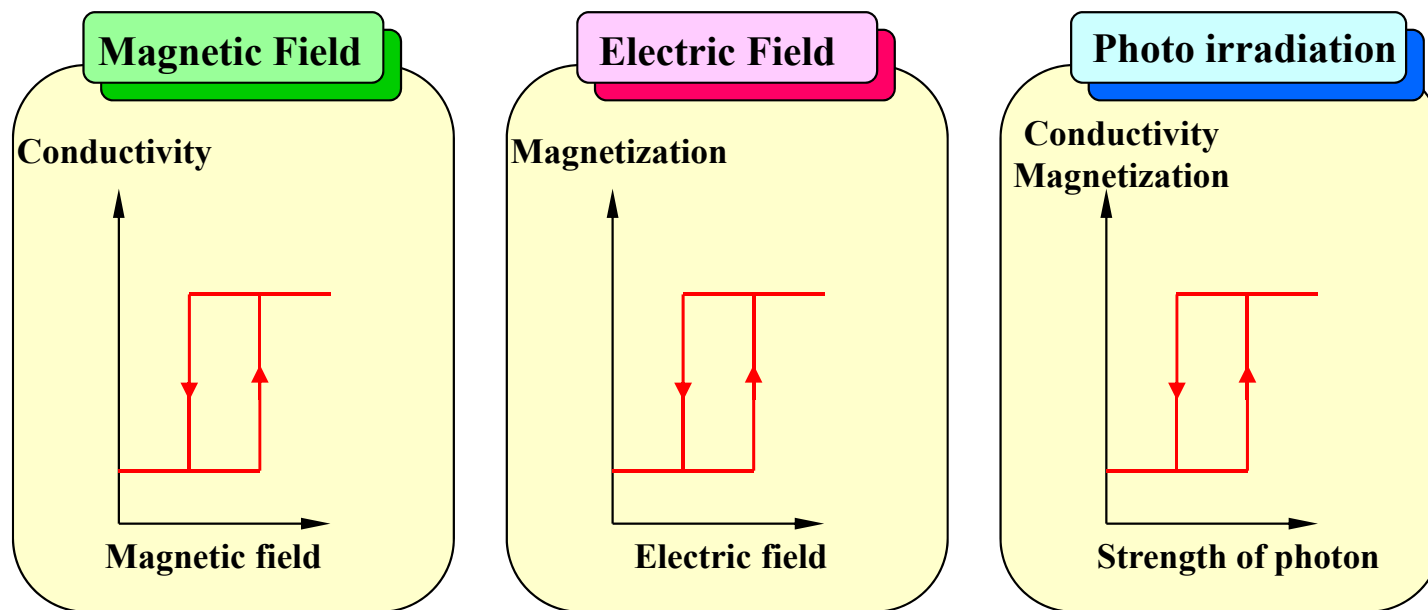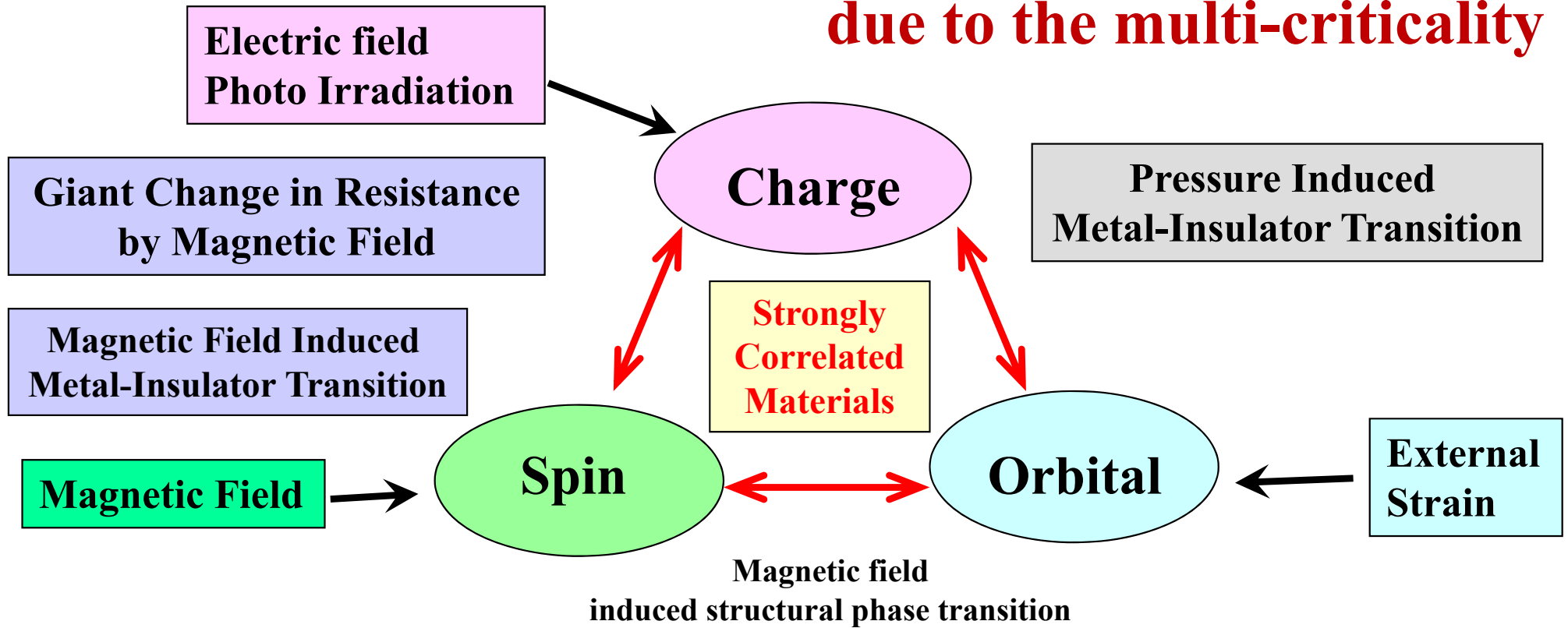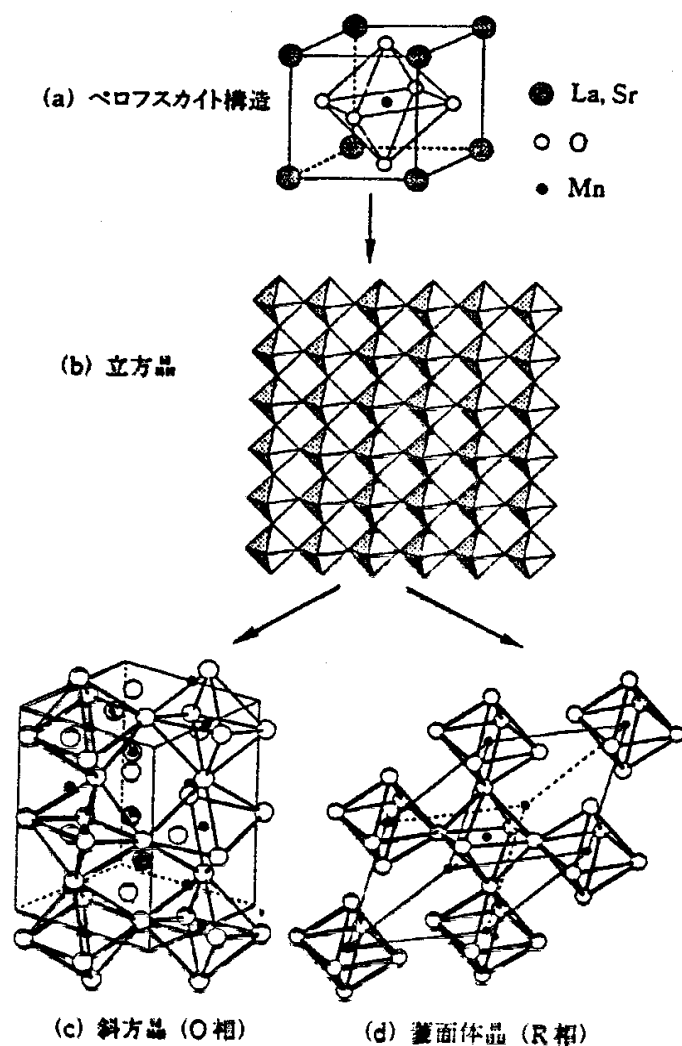$J>0$

$J<0$

(a) 常磁性状態

(b) 強磁性状態

(c) 反強磁性状態

Spin configurations in localized magnetic systems

- Magnetic field control of resistance

- Photo-irradiation control of resistance

- Electric field control of magnetization

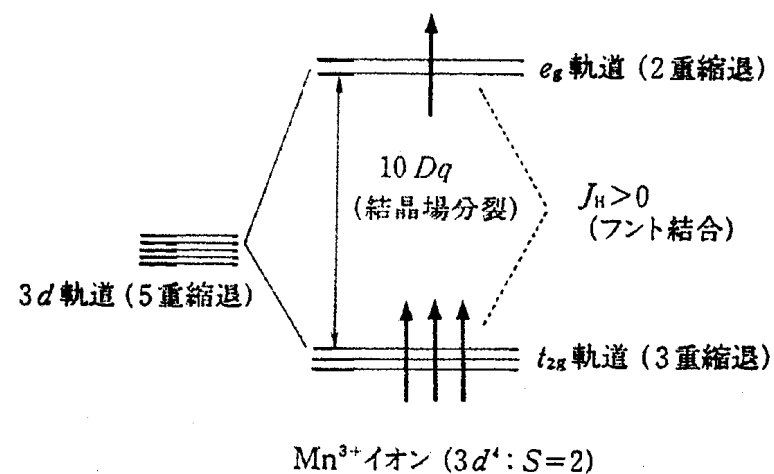# Giant Response to magnetic and electric fields due to the multi-criticality

Electric field Photo Irradiation

Giant Change in Resistance by Magnetic Field

Magnetic Field Induced Metal-Insulator Transition

Magnetic Field

Charge

Pressure Induced Metal-Insulator Transition

Strongly Correlated Materials

Spin

Orbital

External Strain

Magnetic field induced structural phase transition

Magnetic Field

Conductivity

Magnetic field

Electric Field

Magnetization

Electric field

Photo irradiation

Conductivity
Magnetization

Strength of photon

Crystal Structure of Mn Perovskite Oxides
LaMnO$_3$

(a) ペロフスカイト構造

● La, Sr
○ O
• Mn

(b) 立方晶

(c) 斜方晶 (O相)　　(d) 菱面体晶 (R相)

Electronic Strucutre of Mn
Perovskite Oxides

e_g軌道（2重縮退）

$10\,Dq$
（結晶場分裂）

$J_H > 0$
（フント結合）

$3d$軌道（5重縮退）

t_{2g}軌道（3重縮退）

Mn^{3+}イオン（$3d^4$: $S=2$）

第2図　Mn^{3+}イオンの電子状態.
$3d^4$: $t_{2g}{}^3 e_g{}^1$, $S=2$ の高スピン状態をとる.
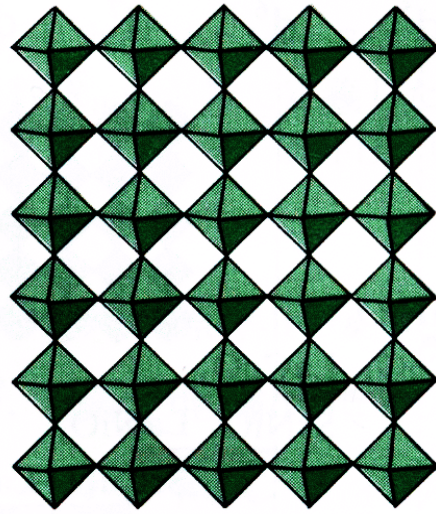
$n = \infty$
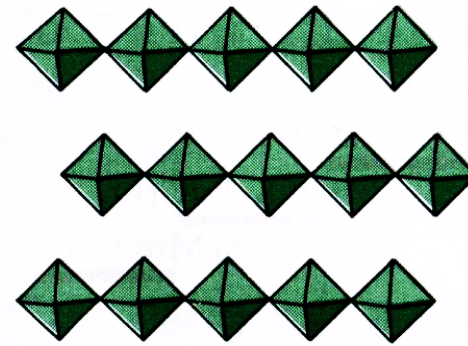
$n = 1$

Transition metal Elements

Oxygen

Rare earth ions

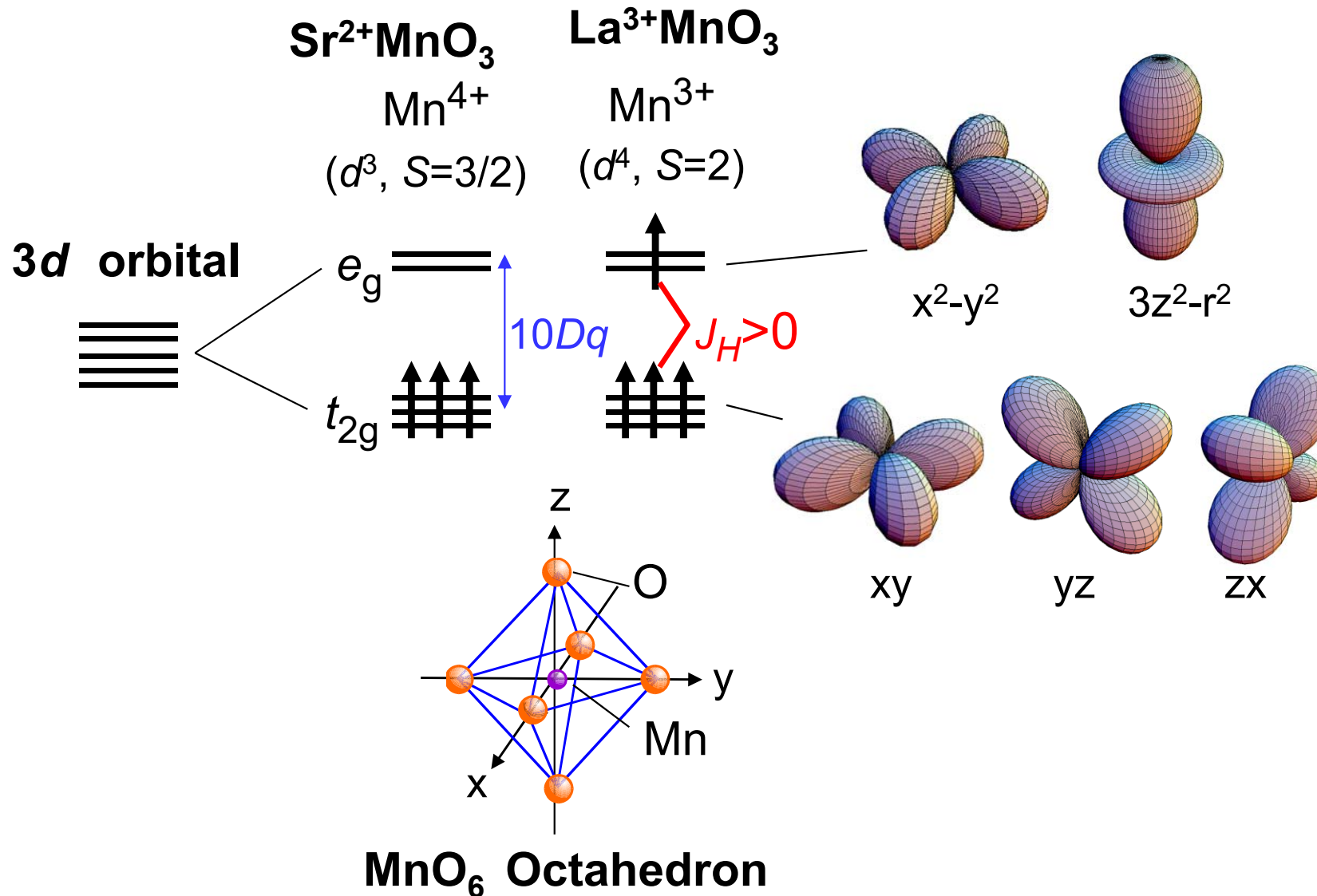A

B

O

(a)

(b)
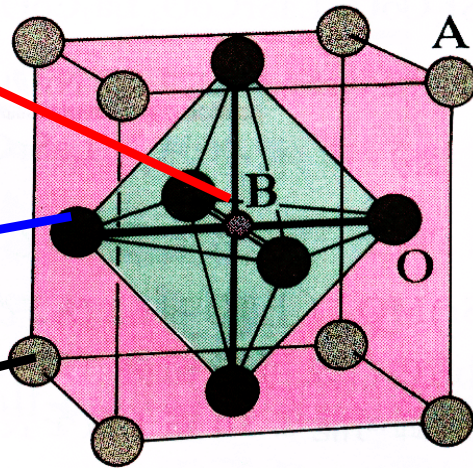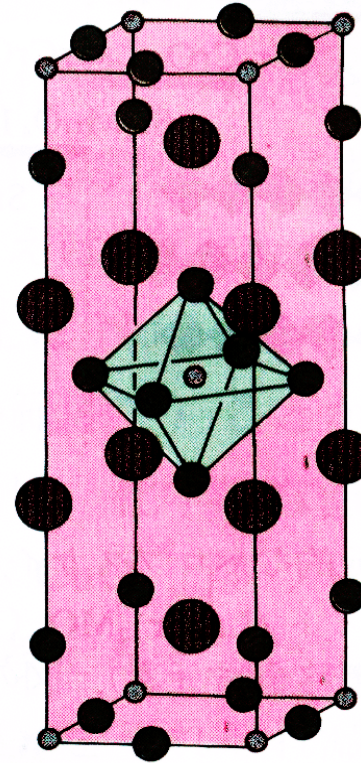
Perovskite

Layered Perovskite

Electronic Structure of Manganese oxides

$Sr^{2+}MnO_3$ $\quad$ $La^{3+}MnO_3$

Mn^{4+} $\qquad$ Mn^{3+}

$(d^3, S=3/2)$ $\quad$ $(d^4, S=2)$

3d orbital

e_g

t_{2g}

$10Dq$

$J_H > 0$

x^2-y^2 $\qquad$ $3z^2-r^2$

xy $\qquad$ yz $\qquad$ zx

z

O

y

Mn

x

MnO_6 Octahedron

Hund's Coupling J_H > CEF splitting 10Dq

By doping, Ferromagnetic metallic state is stabilized

Resistance

Temperature (K)
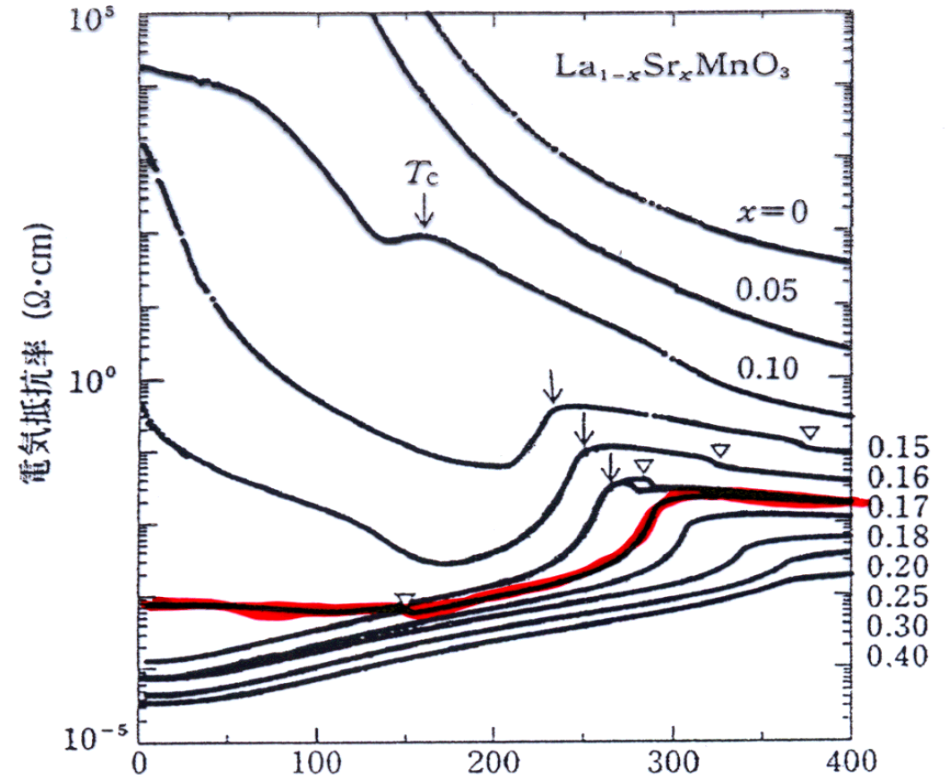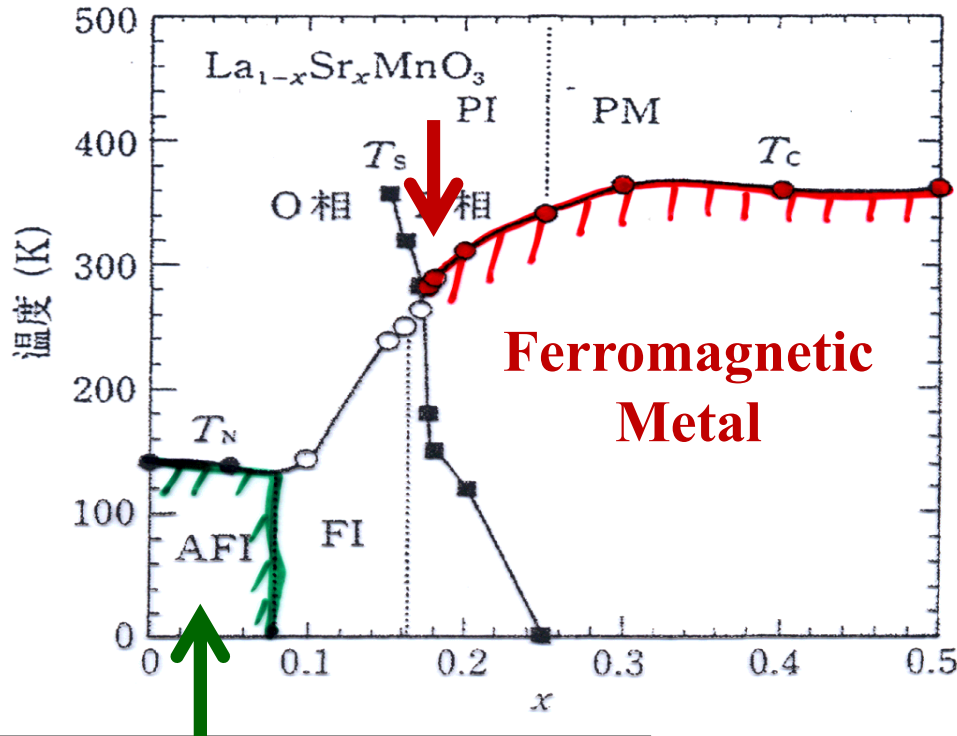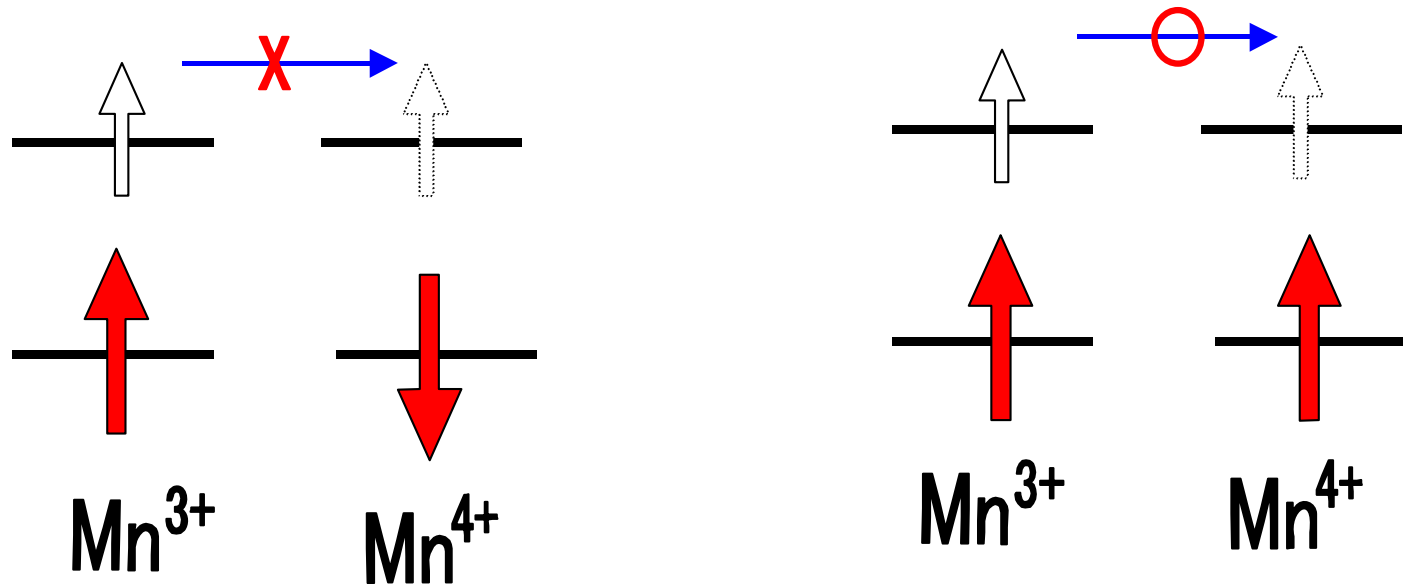
Ferromagnetic Metal

Antiferromagnetic Insulator

Strong coupling of spin and charge degrees of freedom

Hund's coupling

Conduction electrons

Localized spins

$La^{3+}MnO_3$ $Sr^{2+}MnO_3$

Mn^{3+} Mn^{4+}

Mn^{3+} Mn^{4+}
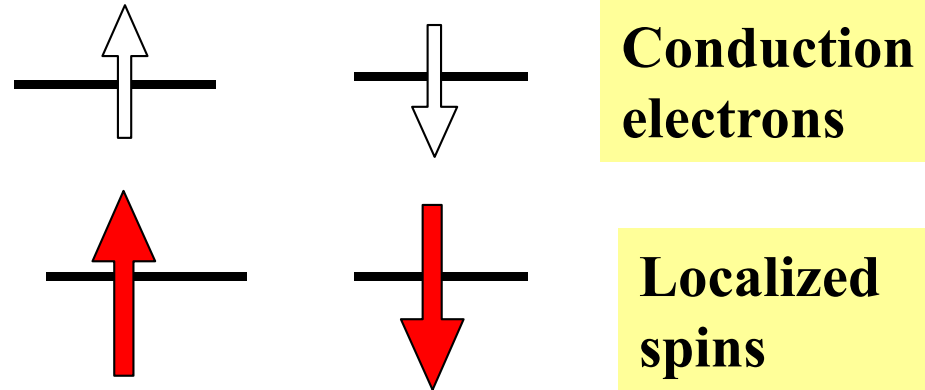
(a) $d\varepsilon$ spins are ferromagnetic, $d\gamma$ electron is mobile.
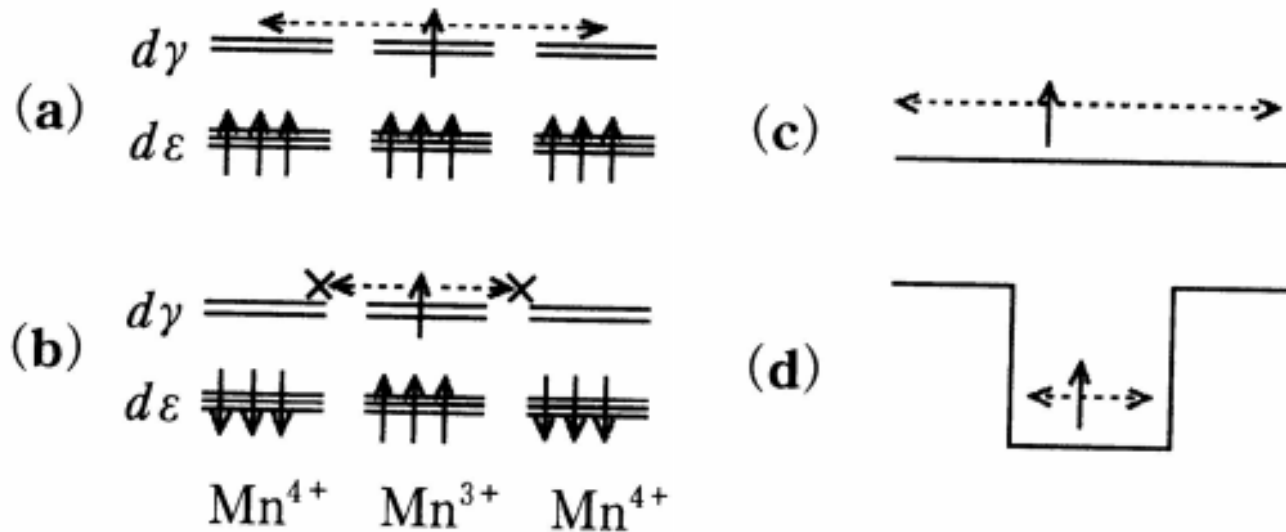
(b) $d\varepsilon$ spins are antiferromagnetic, $d\gamma$ electron is localized.

When J_{ex} is negative due to the overlap of wave functions among nearest neighbor atomic sites, Spins are anti-parallel. On the other hand, if the wave function is orthogonalized, J_{ex} is always positive and hence ferromagnetism is realized

Proof:

$$J_{n_1 n_2} = \int \varphi_{n_1}^*(r_1)\varphi_{n_2}^*(r_2)\frac{e^2}{r_{12}}\varphi_{n_1}(r_2)\varphi_{n_2}(r_1)d\tau_1 d\tau_2$$
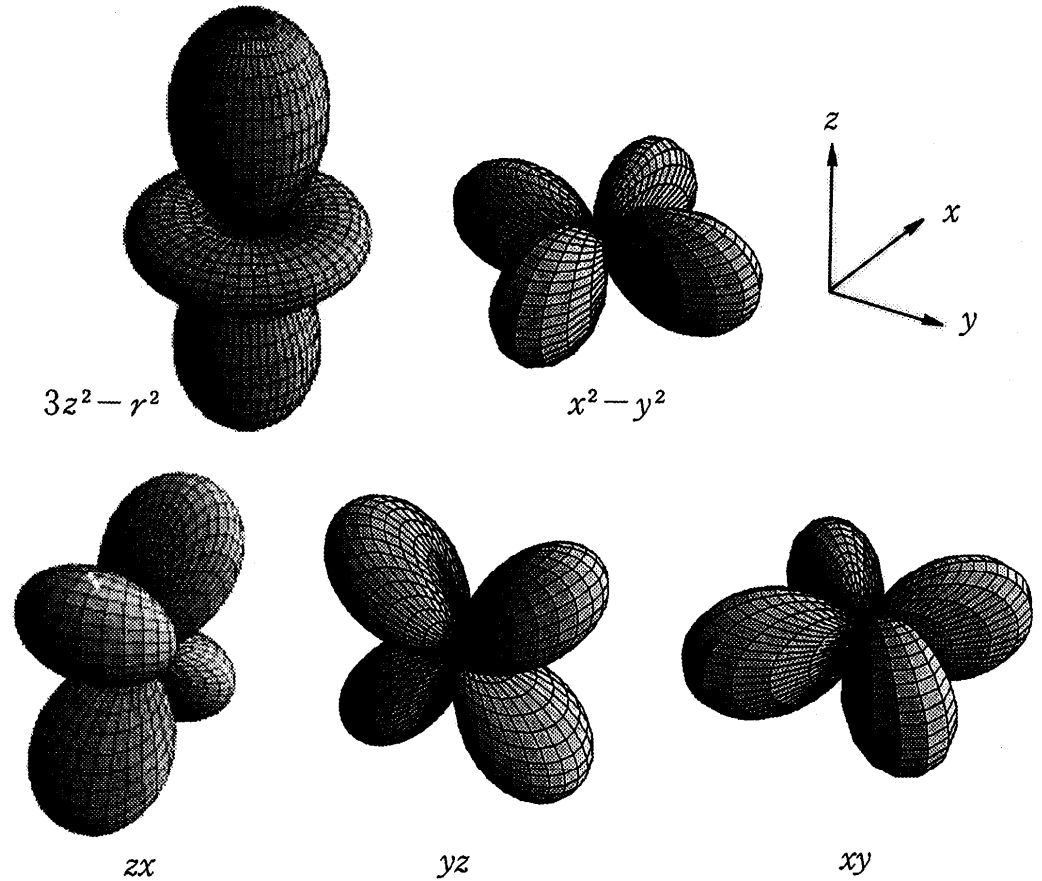
1 / r is expanded in a Fourier series as

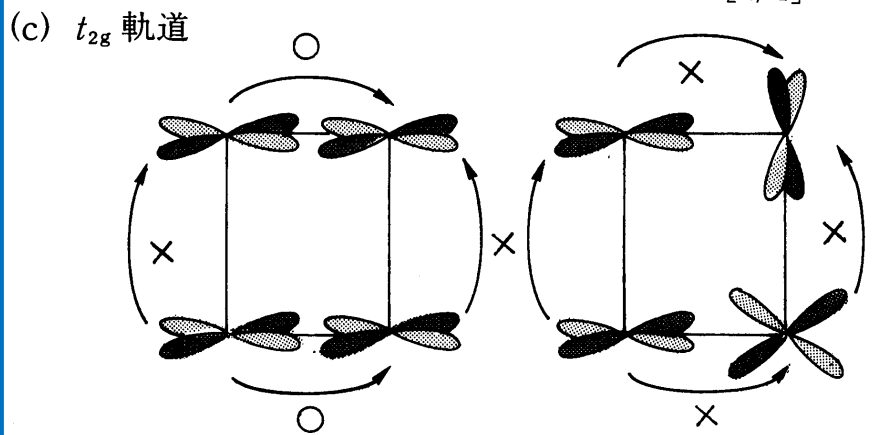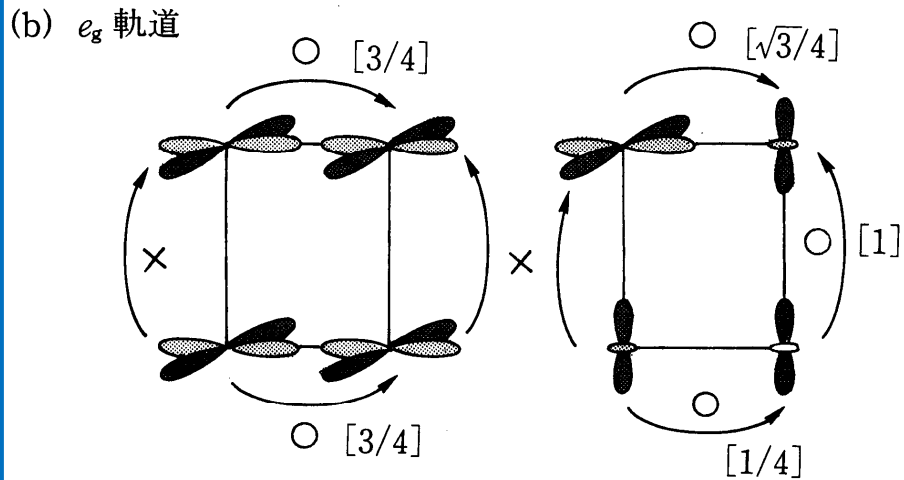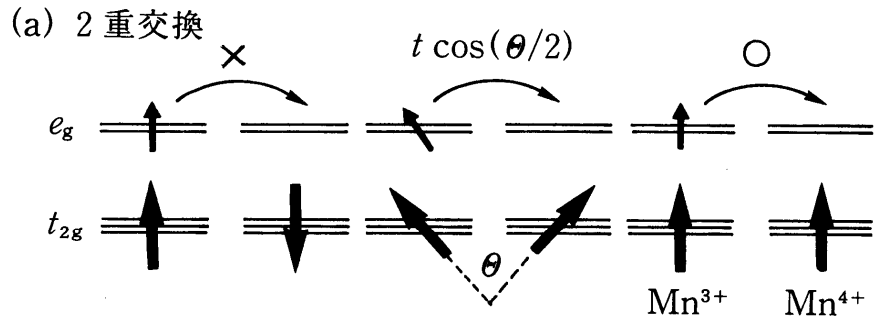$$\frac{e^2}{r_{12}} = \frac{1}{V}\sum_k \frac{4\pi e^2}{k^2} e^{ik\cdot(r_1 - r_2)}$$

$J_{ex} = -2St + J' = J'$ (because of S=0)

$$J_{n_1 n_2} = \frac{1}{V}\sum_k \frac{4\pi e^2}{k^2}\int \varphi_{n_1}^*(r_1)\varphi_{n_2}(r_1)e^{ik\cdot r_1}d\tau_1$$

$$\times \int \varphi_{n_2}^*(r_2)\varphi_{n_1}(r_2)e^{-ik\cdot r_2}d\tau_2 > 0$$

のように書きかえられる. したがって $J_{n_1 n_2}$ は常に正である.

There is a restriction for electrons to transfer depending on spin and orbital states
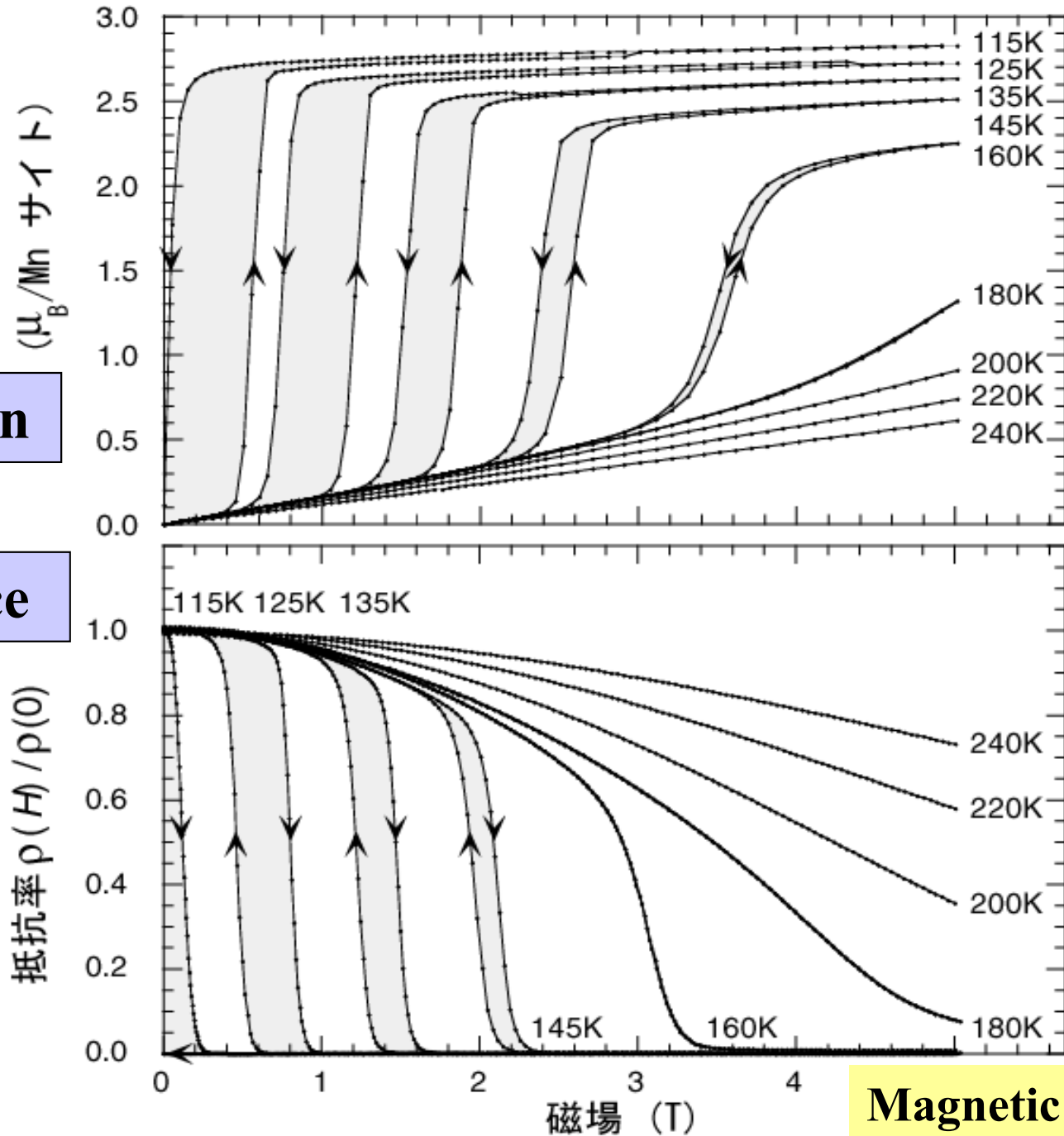
(a) 2 重交換

e_g × $t\cos(\theta/2)$ ○

t_{2g}

θ

Mn³⁺   Mn⁴⁺

(b) e_g 軌道

○ [3/4]   ○ [√3/4]

×   ×   ○ [1]

○ [3/4]   [1/4]

(c) t_{2g} 軌道

○   ×

×   ×   ×

○   ×

$3z^2 - r^2$ $x^2 - y^2$

z

x

y

zx yz xy

第 3 図 d 電子軌道.

CMR effect
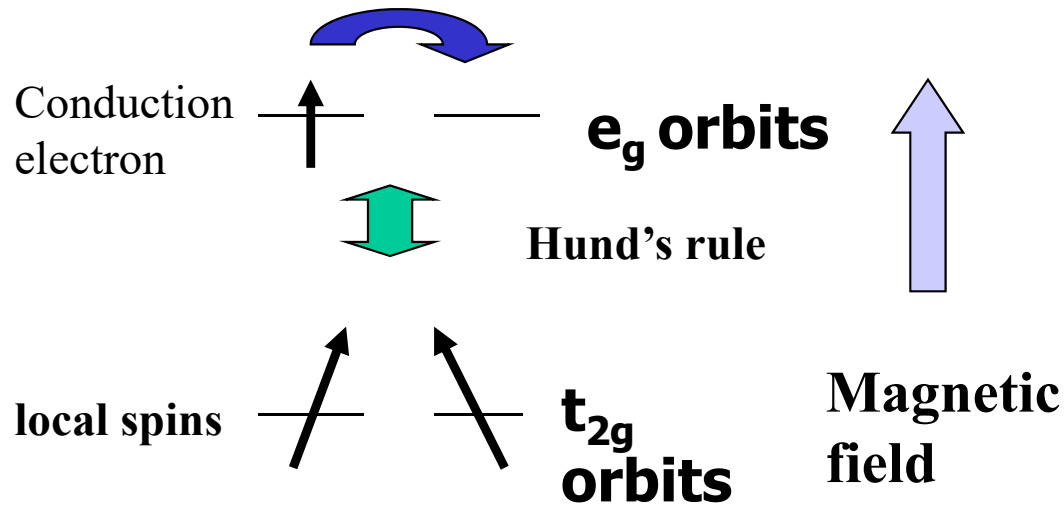
$(Nd,Sm)_{0.5}Sr_{0.5}MnO_3$

Colossal Magneto Resistance

Magnetization

Resistance

Magnetic field

Magnetic Field Control of Magnetic and Transport Properties in $Pr_{1-x}Ca_xMnO_3$

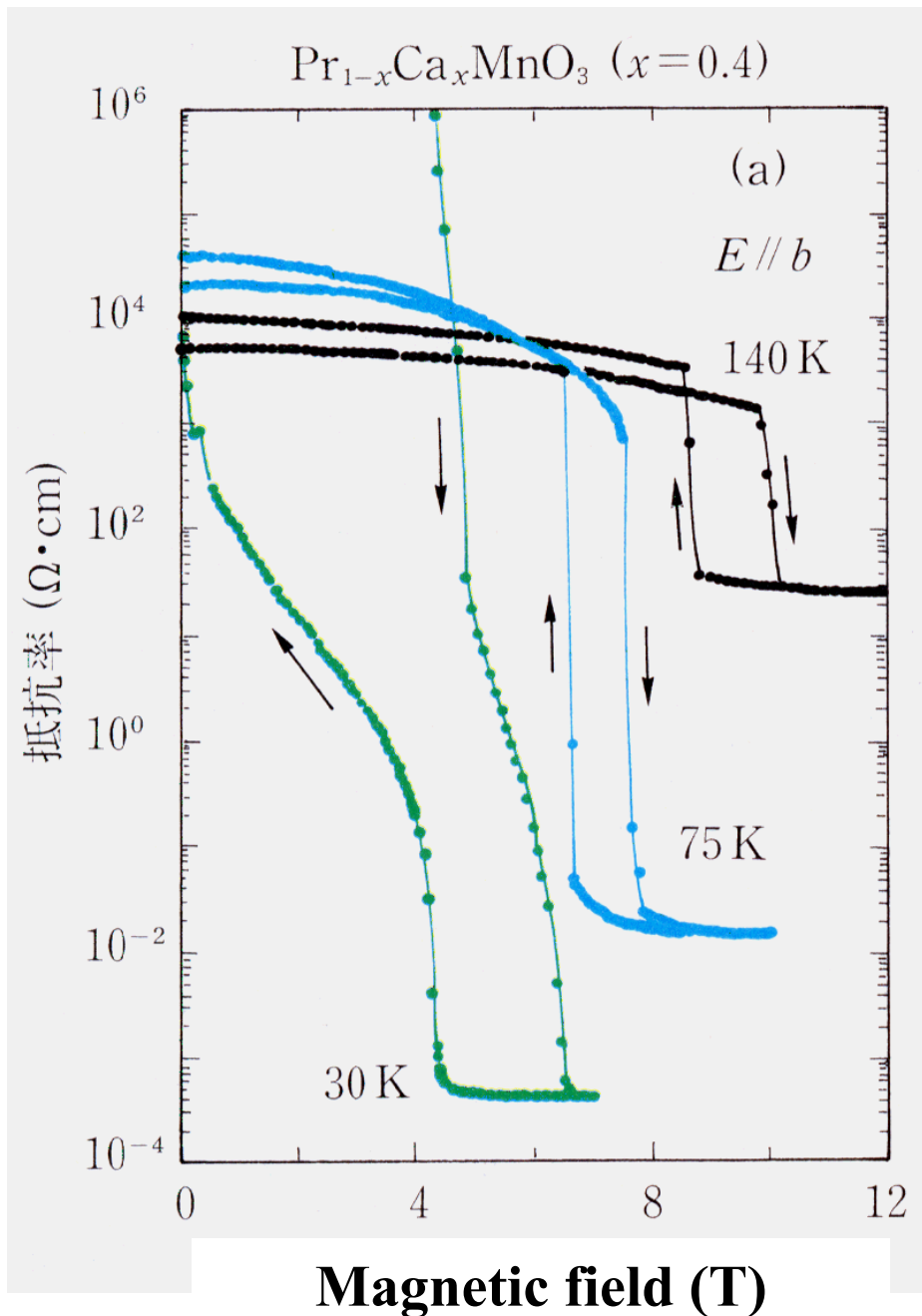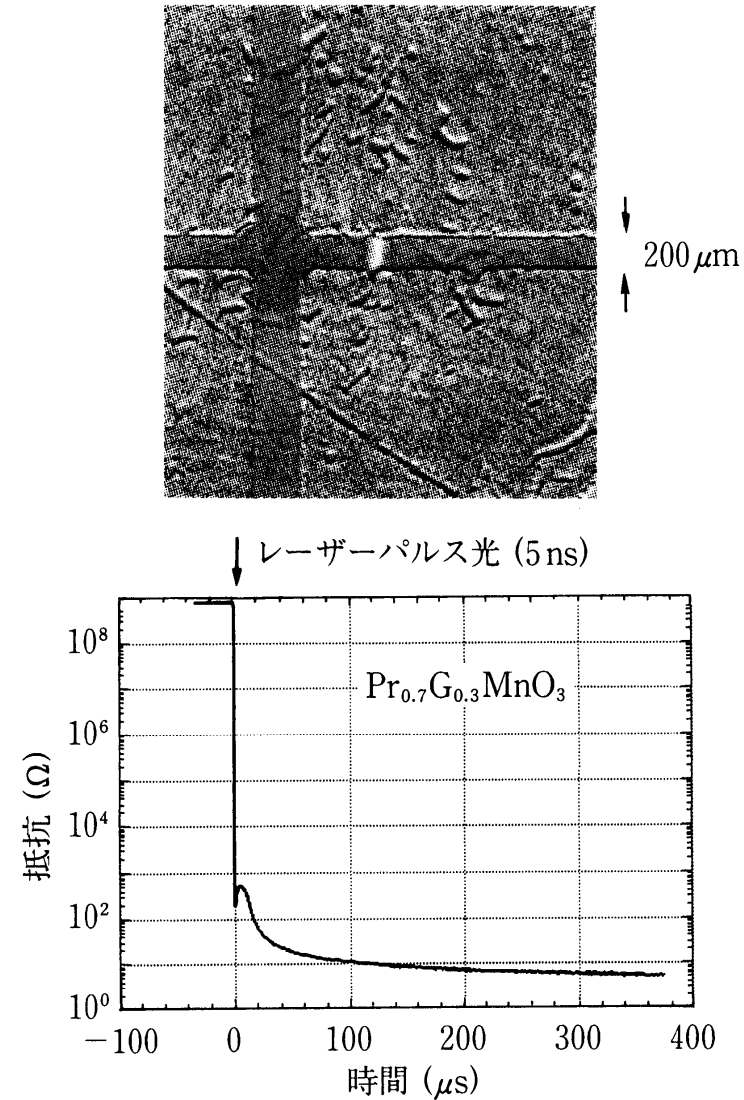**Competition between Ferromagnetic Metallic and charge ordered insulating phases**

Conduction electron

e_g orbits

Hund's rule

local spins

t_{2g} orbits

Magnetic field

Conductivity controlled by Magnetic filed → local spins → mobile electrons

Resistance

Magnetic field (T)
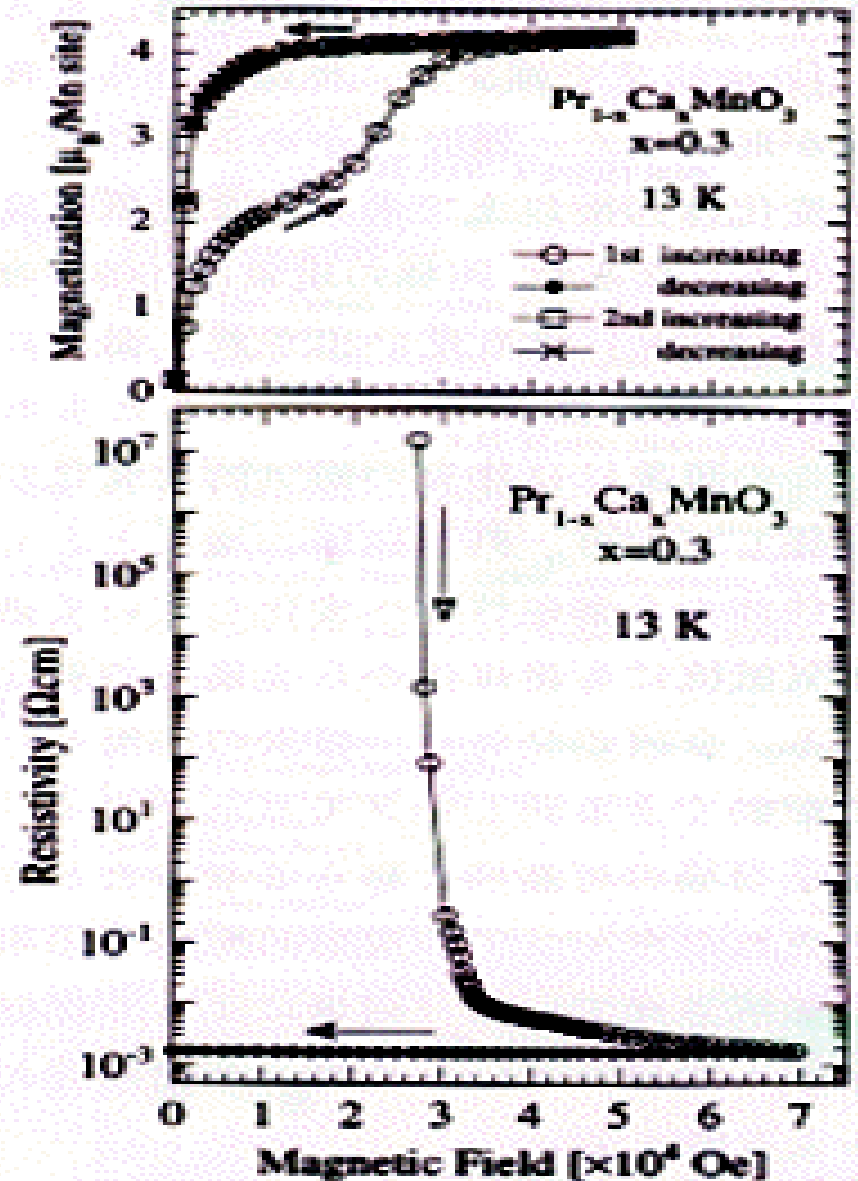
Photo-induced insulator – metal transition
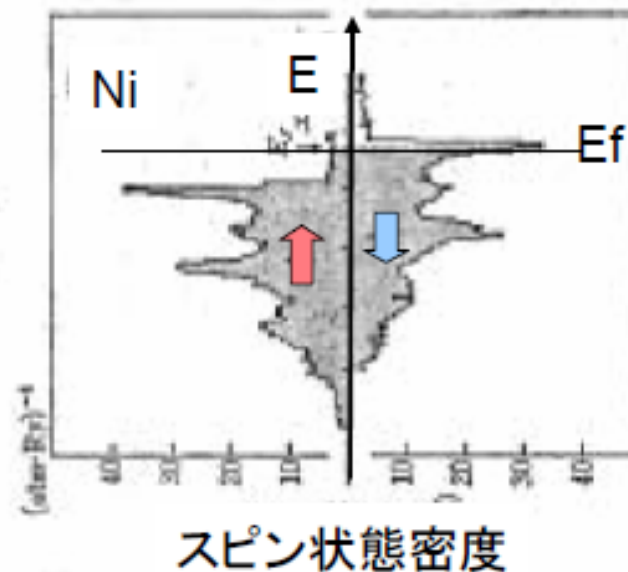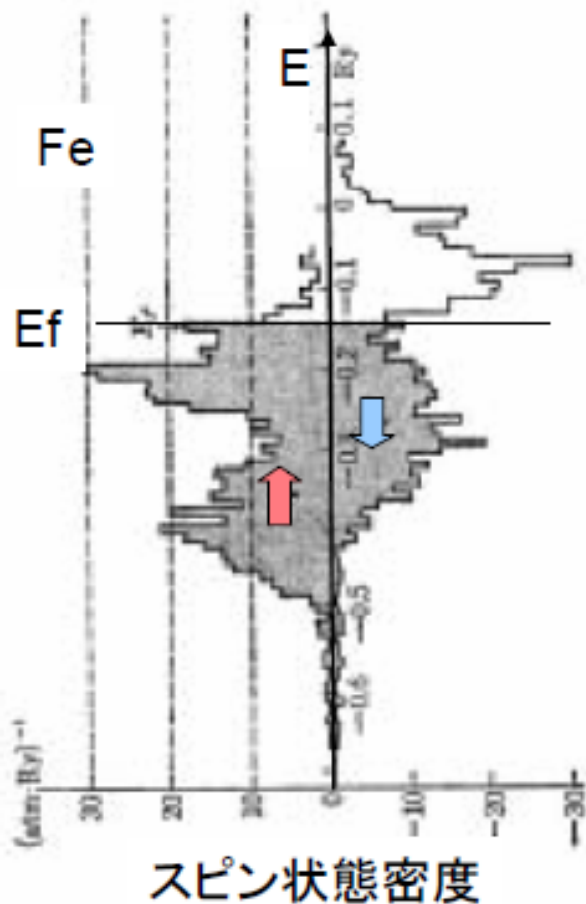

第 8 図　$Pr_{1-x}Ca_xMnO_3$($x=0.3$)結晶のナノ秒パルス光励起に伴う光誘起金属化.

強磁性(Ferromagnetism)

- Ferroというのは「鉄の」という意味で鉄に代表されるような磁気的性質という意味である。
- 鉄に代表される性質とは、外部磁界を加えなくても磁化をもつ、即ち、自発磁化をもつことである。
- 強磁性体の例：

  遷移金属 Fe, Co, Ni,

  遷移金属合金:$Fe_{1-x}Ni_x$, $Fe_{1-x}Co_x$, $Co_{1-x}Cr_x$, $Co_{1-x}Pt_x$, $Sm_{1-x}Co_x$

  金属間化合物：PtMnSb, MnBi, $NdFe_2B_{14}$

  酸化物・カルコゲナイド・ニクタイド、ハライド：
    $La_{1-x}Sr_xMnO_3$, CrO_2, $CdCr_2S_4$, Cr_3Te_4, MnP, $CrBr_3$
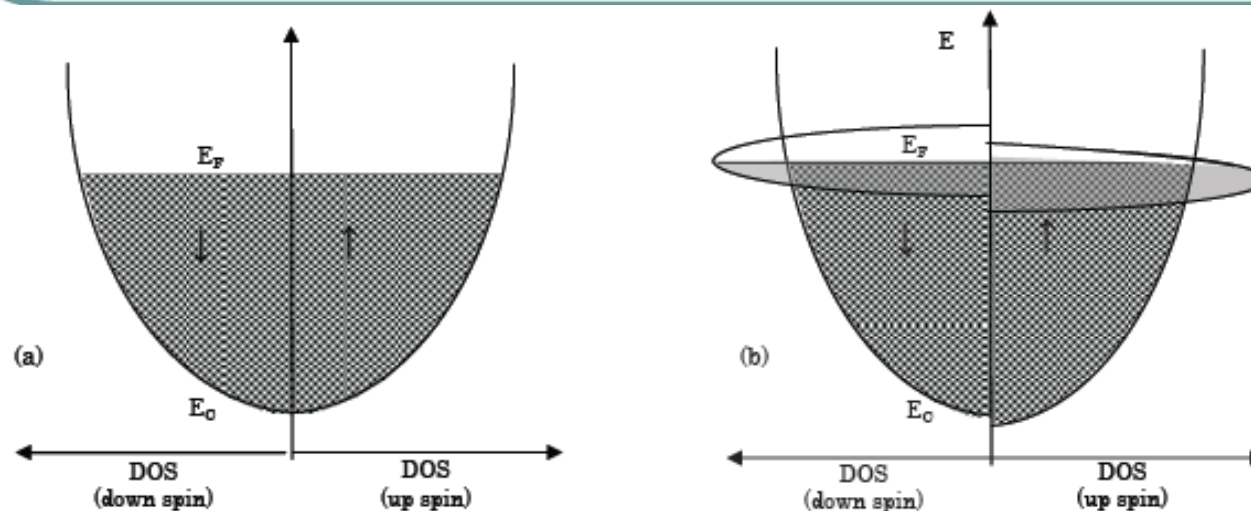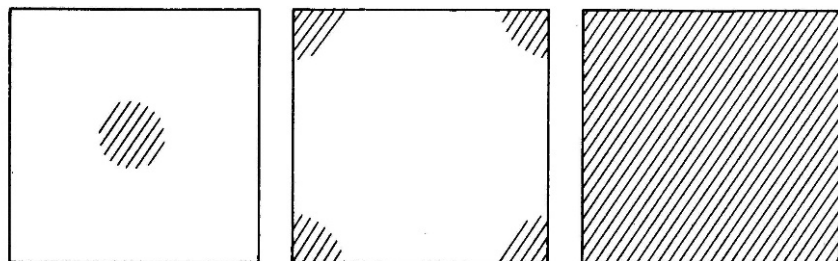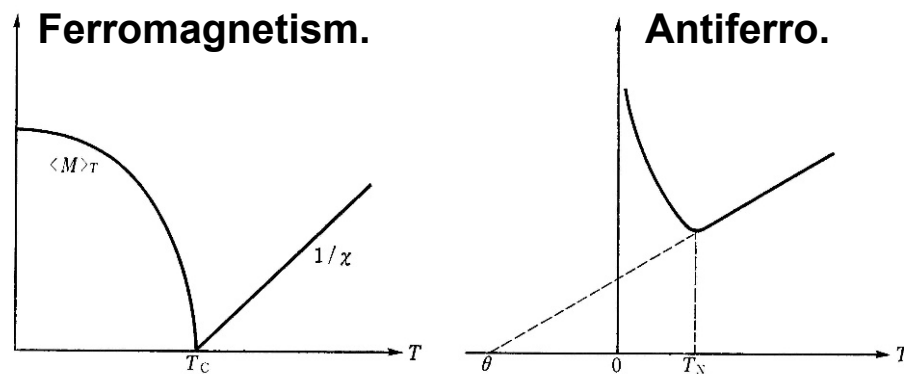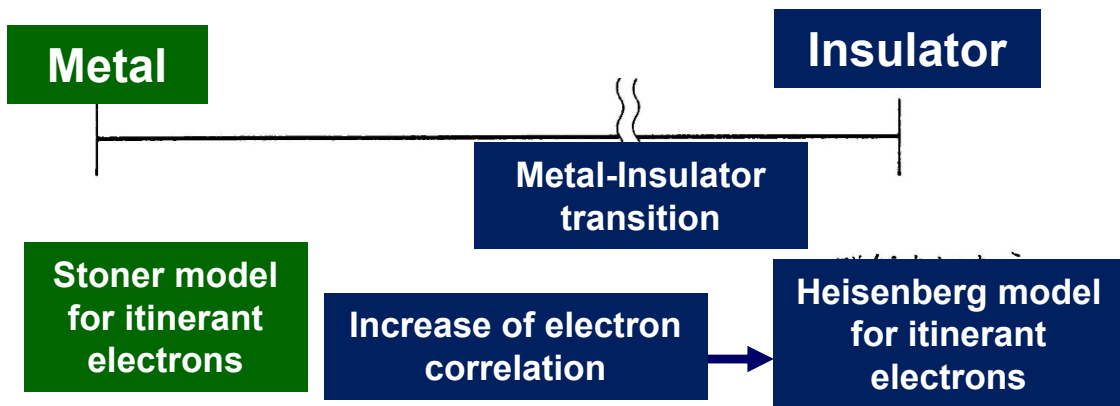
FeとNiの 3d band structures

- Feは↑スピンバンドに比し↓バンドの状態密度がかなり小さい。$n_\uparrow - n_\downarrow = 2.2$

- Niは↑スピンバンドは満ち、↓バンドにはわずかな正孔しかない。$n_\uparrow - n_\downarrow = 0.6$

↓バンドに0.6個の空孔があると、Cuからs電子が流れこみ、Cuが40%合金したときモーメントを失う。

Fe

Ef

スピン状態密度

Ni

Ef

スピン状態密度

Itinerant Magnetism & Spin-fluctuations

Metal

Insulator

Metal-Insulator transition

Stoner model for itinerant electrons

Increase of electron correlation

Heisenberg model for itinerant electrons

Ferromagnetism.

$\langle M \rangle_T$

$1/\chi$

T_C

T

Antiferro.

θ 0 T_N T

Localized magnetism

Weak itinerant Ferro.

Weak itinerant Antiferro.

Localized electrons mag.

Wave-number dependent susceptibility follows a Currie Weiss law in a different origin from the localized model

$$\mathcal{H} = \sum_{i,j,\sigma} t_{ij}\, a^+{}_{i\sigma}\, a_{j\sigma} + U \sum_i n_{i\uparrow} n_{i\downarrow}$$

$$S_{iz} = \frac{1}{2}\,(n_{i\uparrow} - n_{i\downarrow})$$

This relationship replaces the abvoe second term in Hamiltonian to the follows;

$$-2I \sum_i S_{iz}^{\,2} + \text{const}$$

Self-consistent renormalization (SCR) theory:

$$\langle S_{iz}(t) S_{iz}(t') \rangle \sim \langle S_{iz}(t) \rangle \langle S_{iz}(t') \rangle$$

$$\chi(q, \omega) = \frac{\chi_0(q, \omega)}{1 - I\chi_0(q, \omega) + \lambda(q, \omega)}$$

when taking $\langle S_{iz} \rangle$ **=const.**

$$\chi = \frac{2N(E_F)}{(1 - \alpha_0)}$$

$$\alpha_0 = IN(E_F)$$

$$\mathcal{H} = -t \sum_{ij\sigma} c_{i\sigma}^\dagger c_{j\sigma} + U \sum_i n_{i\uparrow} n_{i\downarrow} \tag{5.4}$$

となる．$c_{i\sigma}^\dagger (c_{i\sigma})$ は i 番目の原子軌道上にあるスピン σ をもつ電子の生成 (消滅) 演算子，$n_{i\sigma} = c_{i\sigma}^\dagger c_{i\sigma}$ は粒子数演算子で，その固有値はゼロか 1 である．式 (5.4) の第 1 項の和は最近接原子間についてのみとる．第 2 項は，i 番目のスピンの z 成分を使って，

$$s_{iz} = \frac{1}{2}(n_{i\uparrow} - n_{i\downarrow})$$

と書けるので，

$$s_{iz}^2 = \frac{1}{4}(n_{i\uparrow} - n_{i\downarrow})^2$$

$$n_{i\uparrow} n_{i\downarrow} = -2s_{iz}^2 + \frac{1}{2}(n_{i\uparrow}^2 + n_{i\downarrow}^2)$$

となる．ここで，フェルミ粒子の反交換関係を使って，

$$n_{i\sigma}^2 = c_{i\sigma}^\dagger c_{i\sigma} c_{i\sigma}^\dagger c_{i\sigma} = c_{i\sigma}^\dagger (1 - c_{i\sigma}^\dagger c_{i\sigma}) c_{i\sigma}$$

$$= c_{i\sigma}^\dagger c_{i\sigma} - c_{i\sigma}^{\dagger 2} c_{i\sigma}^2 = c_{i\sigma}^\dagger c_{i\sigma} = n_{i,\sigma}$$

の関係が得られる．ここで，$c_{i\sigma}^{\dagger 2} = c_{i\sigma}^2 = 0$ を用いた．結局，

$$U \sum_i n_{i\uparrow} n_{i\downarrow} = -2U \sum_i s_{iz}^2 + \frac{U}{2} \sum_i (n_{i\uparrow} + n_{i\downarrow})$$

が得られる．この第 2 項の固有値は全電子数 N とすると $(UN/2)$ である
ので，式 (5.4) の第 2 項は，

$$U \sum_i n_{i,\uparrow} n_{i,\downarrow} = -2U \sum_i s_{iz}^2 + \text{const} \tag{5.5}$$

の形に書ける．

相互作用の効果を見るために，式 (5.5) の s_{iz} の一方を熱平均値で $\langle s_{iz} \rangle$ と見なすと，磁化率はパウリの磁化率 $\chi_{\mathrm{P}} = 2\mu_B^2 N(E_{\mathrm{F}})$ を使って，外部磁場 H_0 のもとでの磁化 M は，

$$M = Ng\mu_B \langle s \rangle = \chi_{\mathrm{P}} \left[H_0 + 2UM/(Ng^2\mu_B^2) \right]$$

と得られ，相互作用がある場合の分子場近似の磁化率 χ は，

$$\chi = \frac{\chi_{\mathrm{P}}}{1 - IN(E_{\mathrm{F}})} = \frac{\chi_{\mathrm{P}}}{1 - I\chi_{\mathrm{P}}/(2\mu_B^2)}$$

となる．ここで，$I = U/N$ で N は電子数．この近似では，スピンの揺らぎは取り入れられていないが，$\alpha_0 = IN(E_{\mathrm{F}})$ と表すとき，$\alpha_0 > 1$ のとき，χ が発散し，遍歴強磁性になる．$\alpha_0 < 1$ のとき，パウリの磁化率 χ_{P} は $1/(1 - \alpha_0)$ の因子だけ増大する．$\alpha_0 = 1$ は強磁性発現のストーナー (Stoner) 条件として知られている．

ハーフメタルとは？ What is a half metal ？

(a)

E

E_F

↓ ↑

E_C

DOS
(down
spin)

DOS
(up spin)

(b)

E

↓

E_F

↑

↓

E_C

DOS
(down spin)

DOS
(up spin)
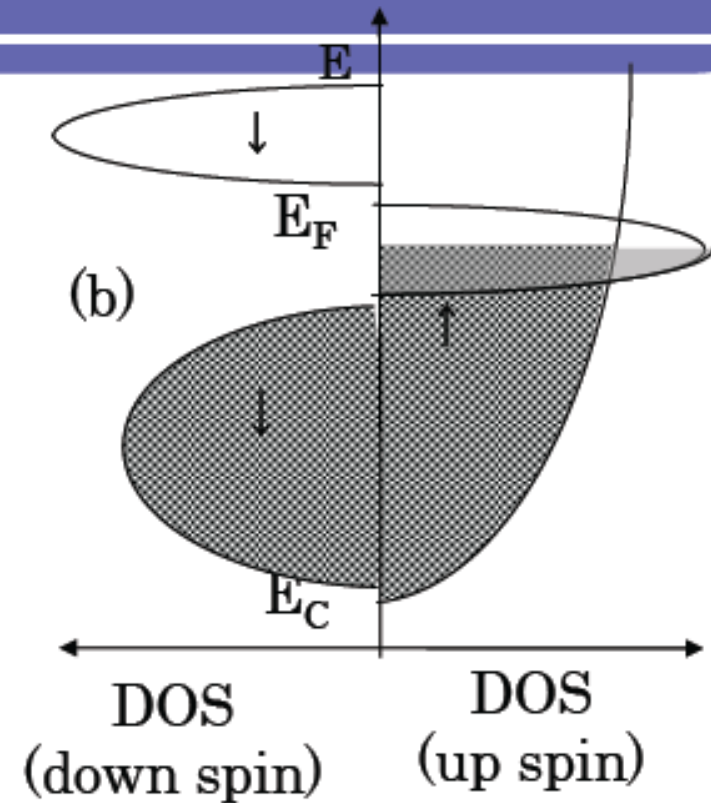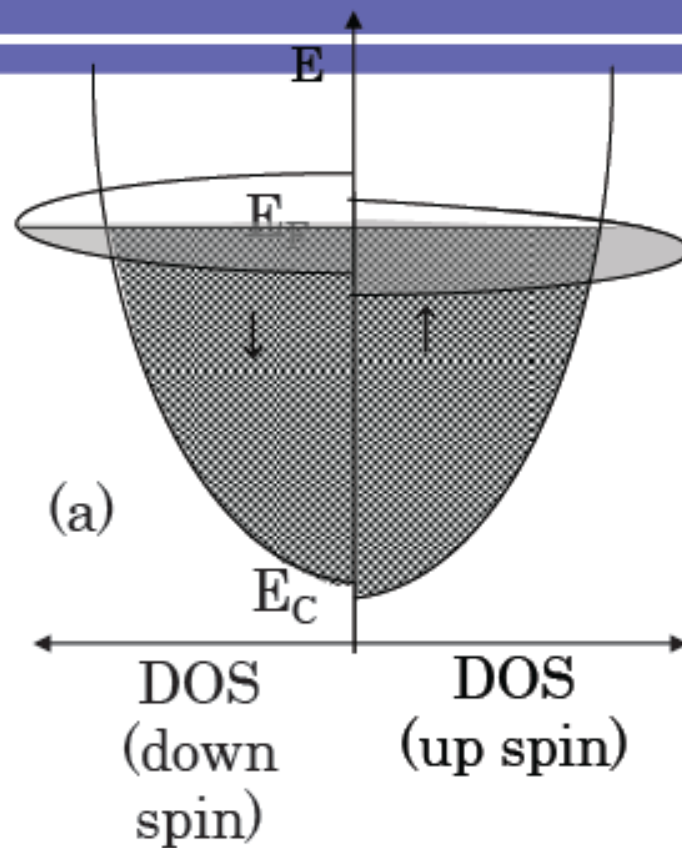
(a)通常の強磁性体金属はup spin, down spinとも金属的
(b)Half metalではup spinは金属、down spinは半導体

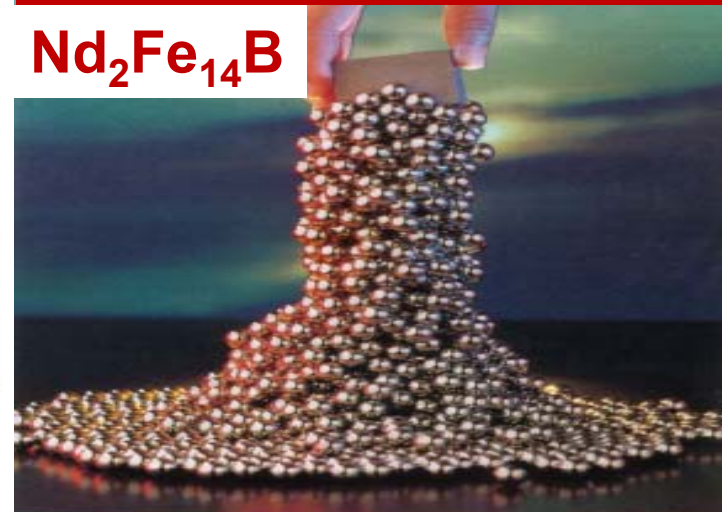# 強相関効果は本当に役に立ち

Ferromagnetic metal
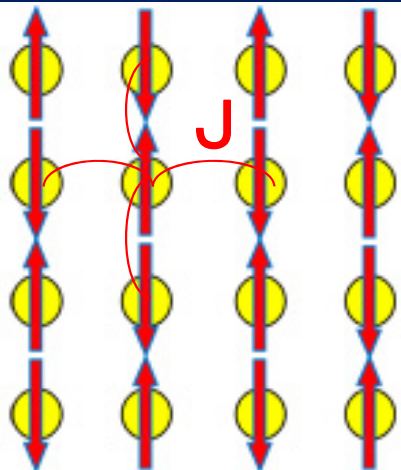
Fe
T_c=1053 K

E_F

Spin Density of States
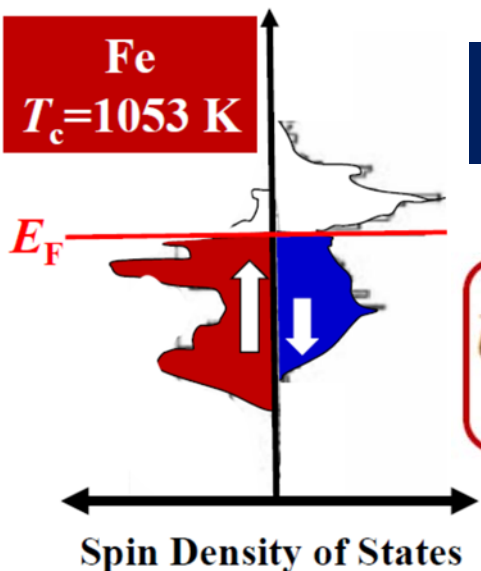
$t \geq U_{eff}$

$T_c\sim1000K$

$$U \sum_i n_{i,\uparrow} n_{i,\downarrow} = -2U \sum_i s_{iz}^2$$

High-performance Permanet Magnet

$Nd_2Fe_{14}B$

Antiferromagnetic Mott Insulator

J

$t << U$

$T_c\sim150$ K

All spins become anti-parallel
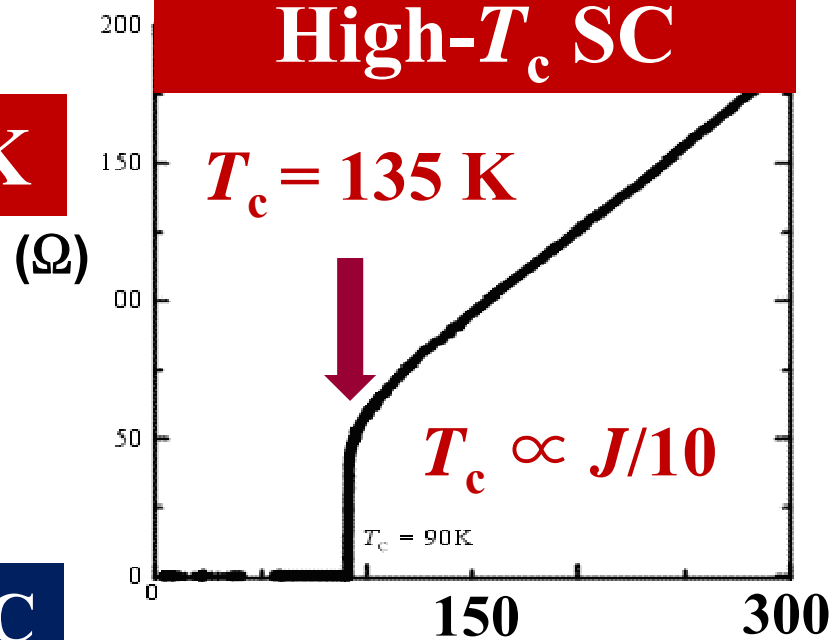
A Route to Search Room-temperature SC

High-T_c SC

(Ω)

$T_c = 135$ K

$T_c \propto J/10$

$T_c = 90K$

200

150

00

50

0

150   300

科学的課題：電子状態の可視化と制御から創発する知と機能

植物

光合成（Ⅱ）活性中心 マンガン磁性錯体

● :Mn原子(spin)

$$2H_2O \longrightarrow O_2 + 4e + 4H^+$$
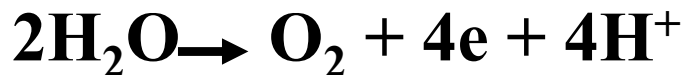
Mn電子スピン状態の 4段階にわたる変化

ミクロ構造がマクロ物性機能を発出

ネオジウム 永久磁石

CRL

半導体：集積回路素子

スピン超格子

スピン軌道作用に よる多様性
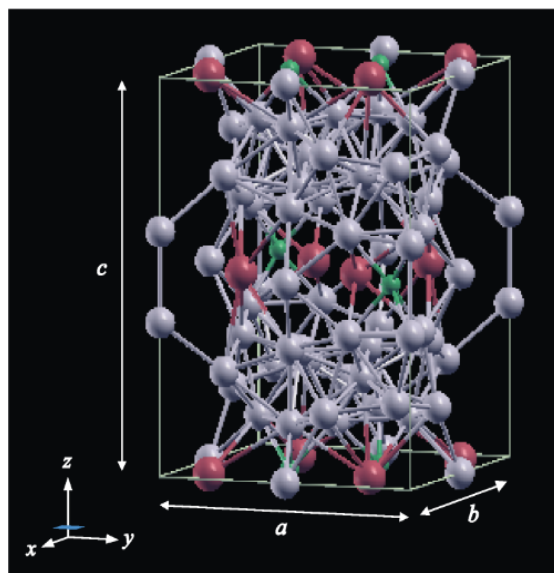
多層系銅酸化物 高温超伝導物質 $T_c = 135\ K$
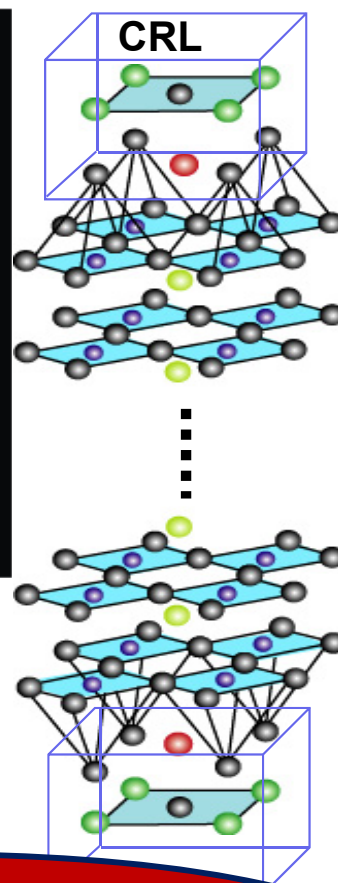
電子の間に働く反発力と 低エネルギー電子移動
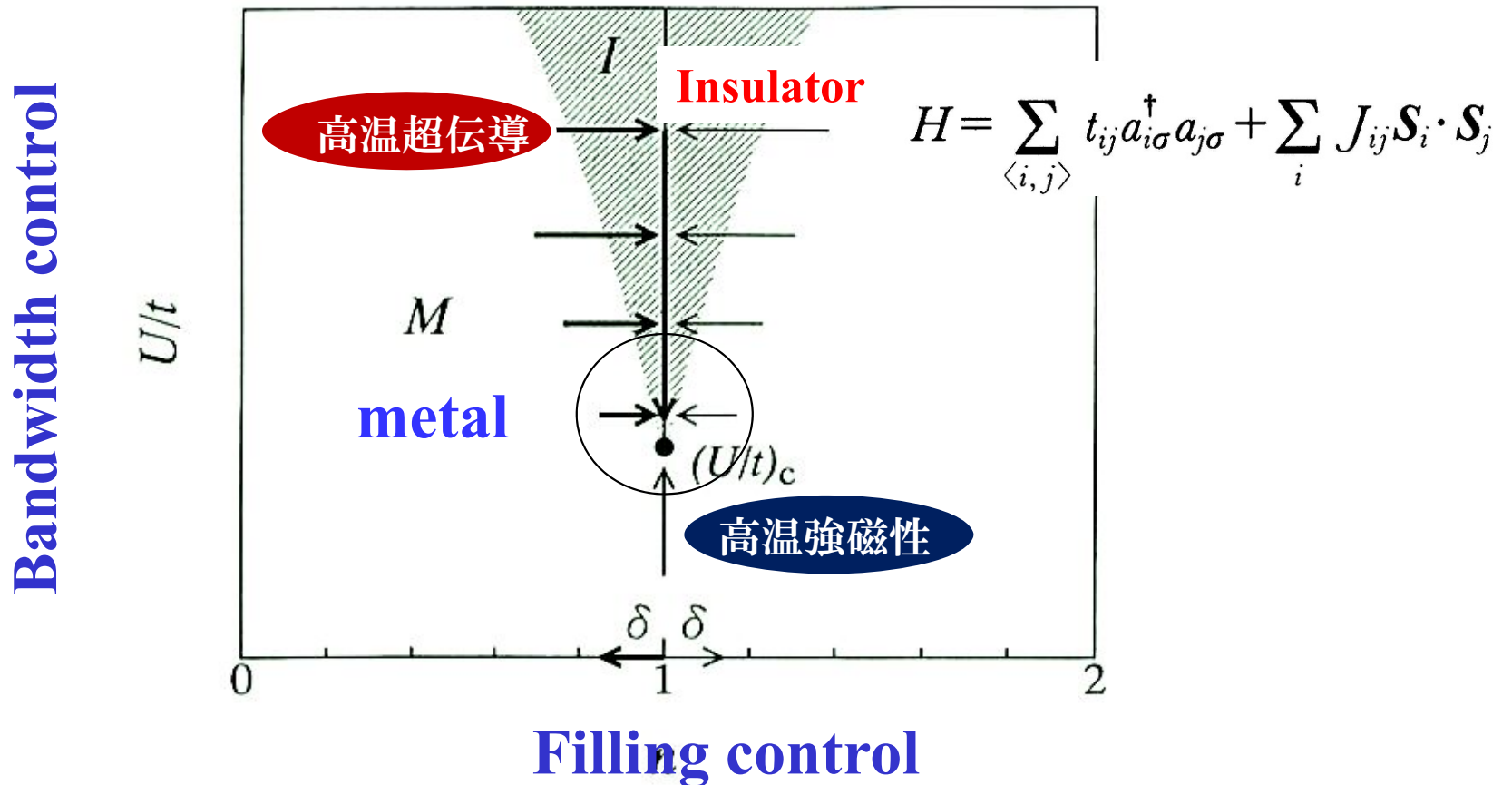
「モノ」の多様性と普遍的な「学理の探究」と「知の活用」

強相関効果は機能を生み出す

Hubbard model

$$H = -t\sum a^+_{i+1} a_i + U\sum n_{i\uparrow} n_{i\downarrow}$$

Kinetic energy　　　　　　　**On-site Coulomb repulsive interaction**
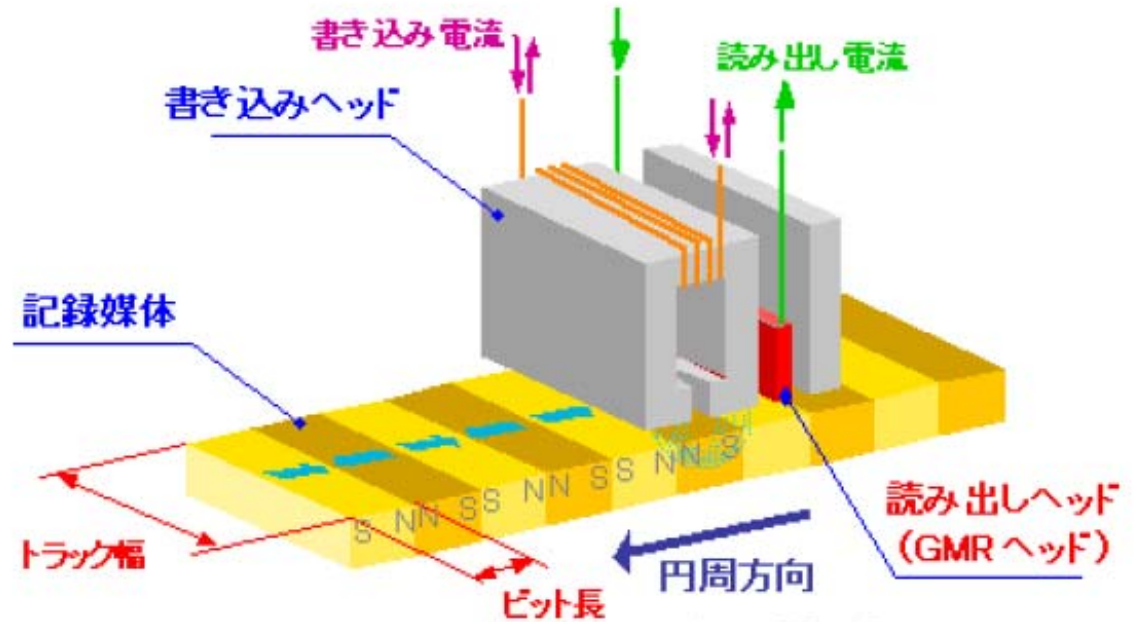
To see outside world　　　　**Make them away from each other**

$$H = \sum_{\langle i,j \rangle} t_{ij} a^\dagger_{i\sigma} a_{j\sigma} + \sum_i J_{ij} S_i \cdot S_j$$

Bandwidth control

U/t

I

Insulator

高温超伝導

M

metal

$(U/t)_c$

高温強磁性

δ　δ

0　　　　1　　　　2

Filling control

スピントロニクスとは

Application of Magneto-resistive effect
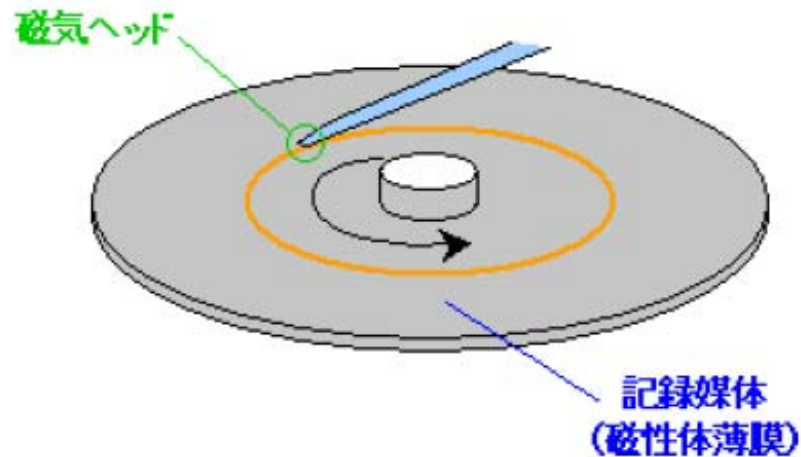
Structure of HardDisc

Magneto-resistivei device structure

(a) 強磁性トンネル接合（MJT）
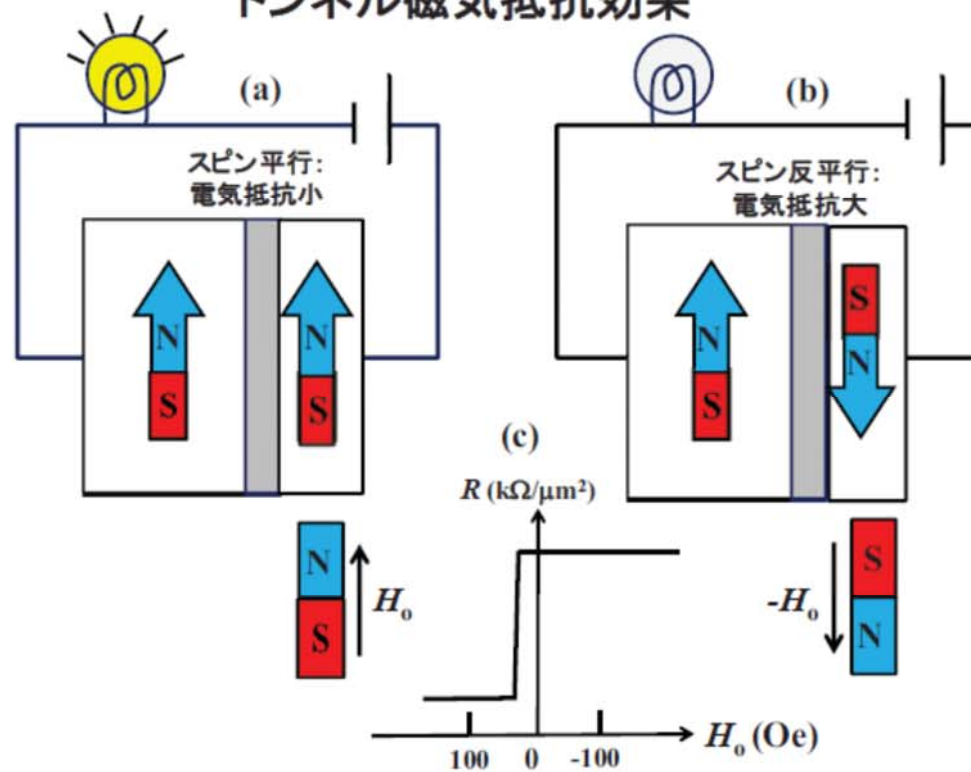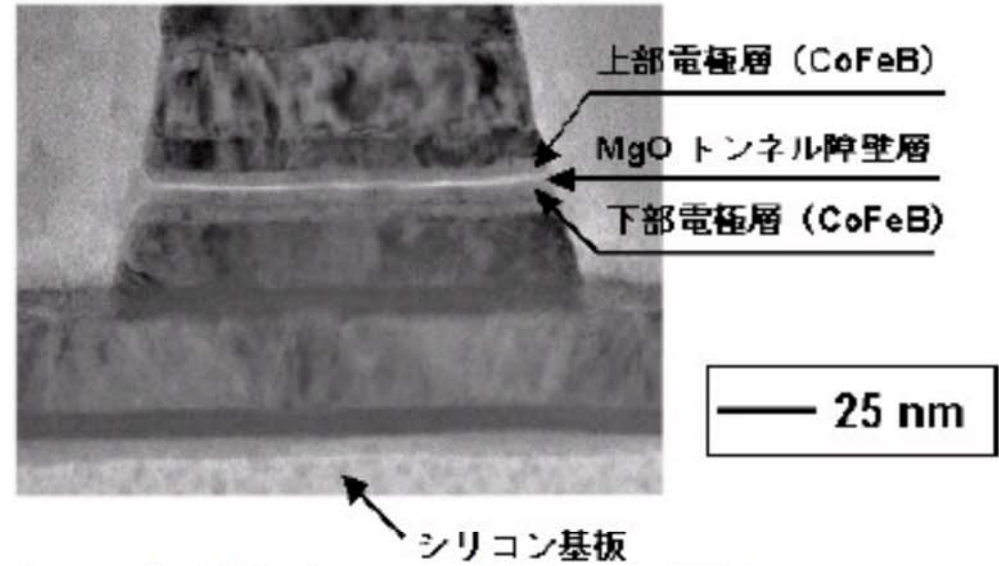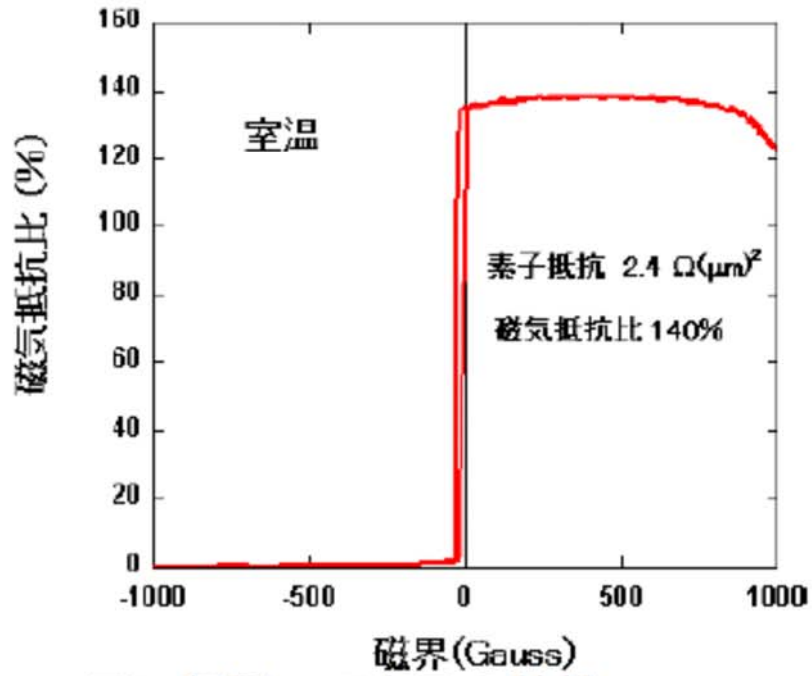
強磁性薄膜
FM1

トンネル障壁（絶縁層）

強磁性薄膜
FM2

(b) トンネル磁気抵抗効果
（TMR効果）

R

R_{AP}

R_P

H

トンネル磁気抵抗効果

(a)

スピン平行：
電気抵抗小

N

S

(b)

スピン反平行：
電気抵抗大

N

S

N

S

(c)

$R\ (k\Omega/\mu m^2)$

N

S

H_o

S

N

$-H_o$

100　　0　　-100　　　$H_o\ (Oe)$

Characteristics of New type of Tunnel magneto-resistive (TMR) device, demonstrating a giant TMR ratio;
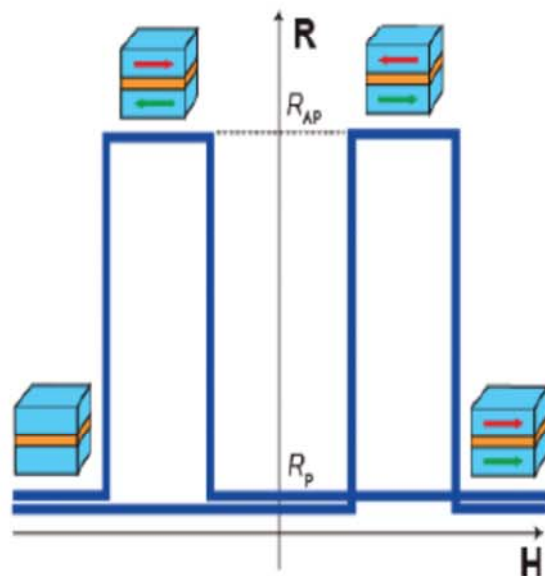
Microscope-image of TMR device
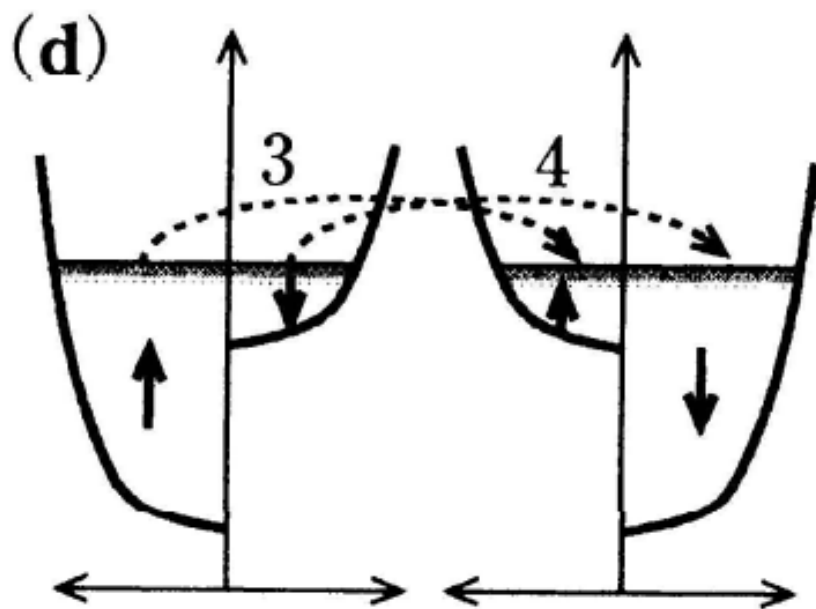
$$TMR = \frac{\rho_{AF} - \rho_F}{\rho_F} = 140\ \%$$
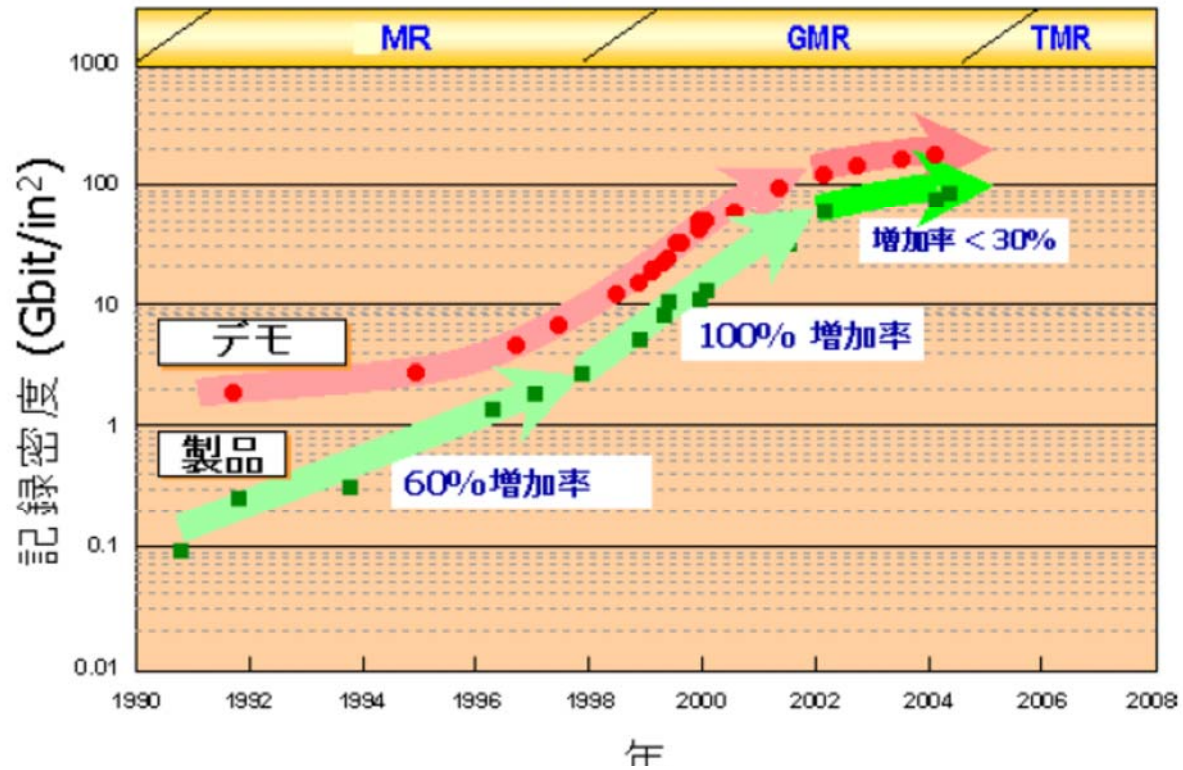
History of increasing memory density with year
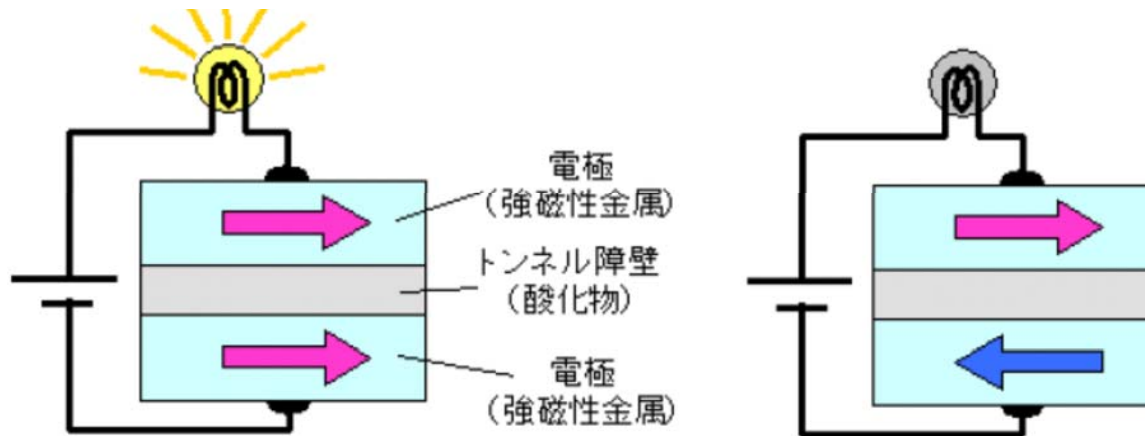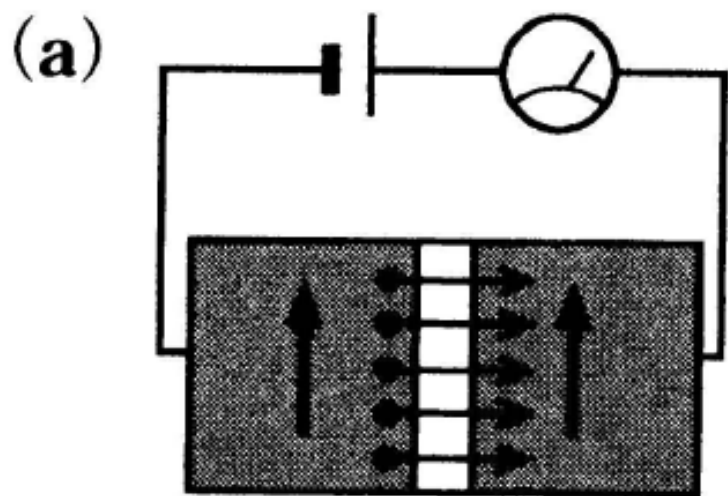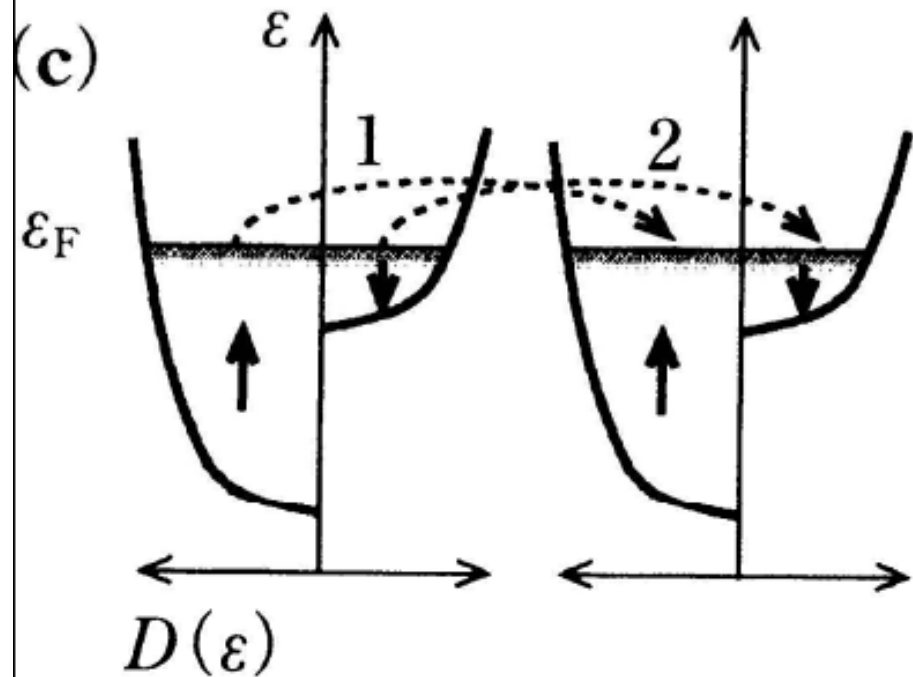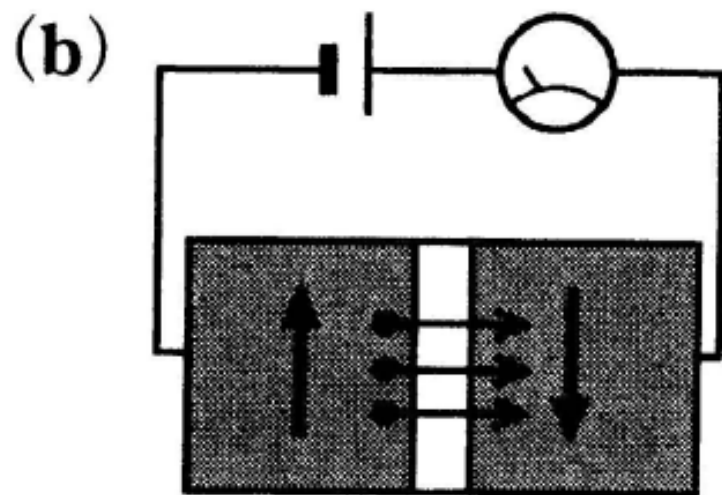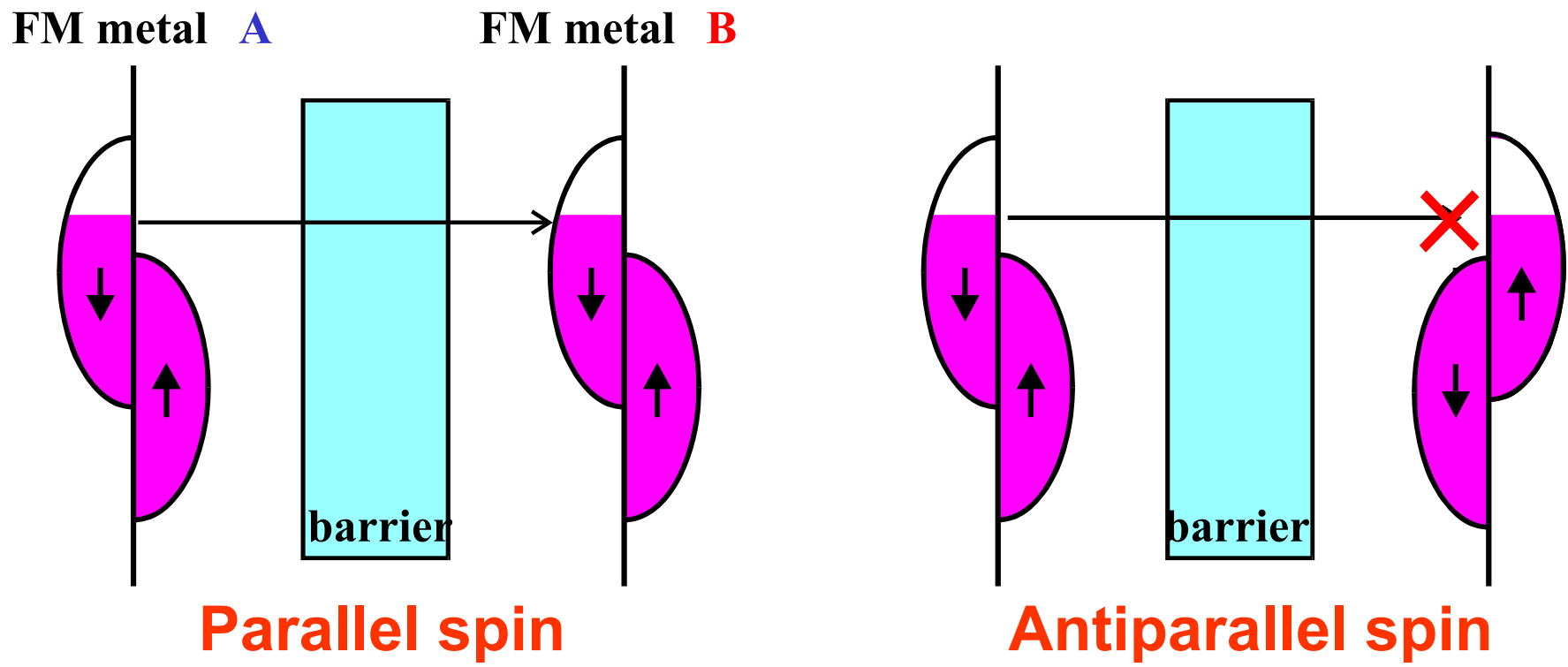
(a) 金属A 絶縁体 金属B

(c) ε, $D(\varepsilon)$, ε_F, 1, 2

(d) 3, 4

トンネルする電子のコンダクタンス G(電気抵抗の逆数) は強磁性層が平行の時，G_P は上向きスピンの状態数の積と下向きスピンの状態数の積の足し合わせで

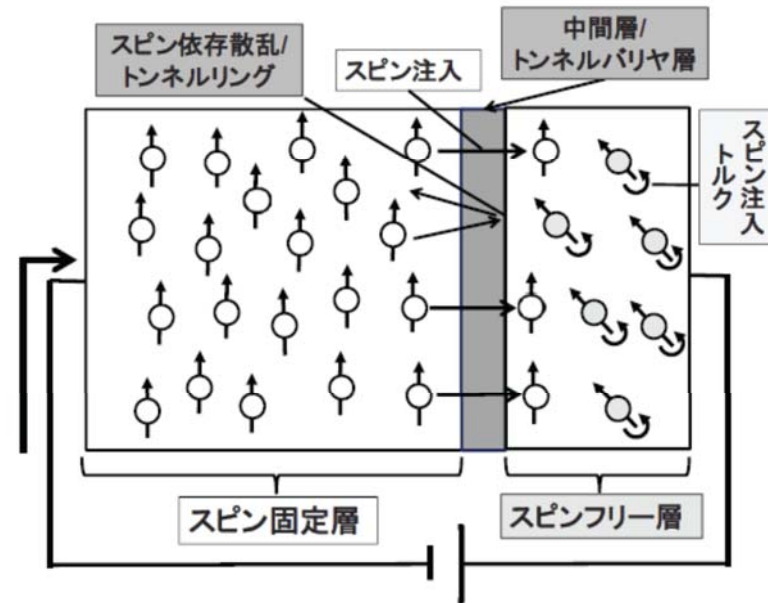$$G_P \propto D_{1M}D_{2M} + D_{1m}D_{2m}$$

と書け，反平行の時，G_{AP} とすると，

$$G_{AP} \propto D_{1M}D_{2m} + D_{1m}D_{2M}$$

となるので，2 つの強磁性層の磁化が平行と反平行のときでは，コンダクタンスに差異が生じる．また TMR 比は，

$$R_{TMR} = \frac{R_{AP} - R_P}{R_P} = \frac{G_P - G_{AP}}{G_{AP}}$$

ている．　特に，巨大磁気抵抗効果はハード磁気ディスクや磁気 RAM の
記録の読出しに利用されている．また，スピン注入トルクによる磁化反転
効果は，磁場を用いない省エネルギー型 MRAM における記録の書き込み
技術として利用されている．

スピントルクダイオード効果

(a)

バイアス・ターミナル

$+I$

上部電極

Cap
CoFeB(3)
MgO(0.85)
CoFeB(3)
Ru(0.85)
CoFe(2.5)

絶縁体

PtMn(15)

下部電極

直流電圧計

マイクロ波発振器

(b)

直流電圧 (μV)

100 Oe   200 Oe   300 Oe   400 Oe   500 Oe   600 Oe

周波数 (GHz)